

# Exploring Halloysite Nanotube and Halloysite Nanotube-Graphene Oxide Composite Material as Carriers for Anticancer Drugs

A Thesis

Submitted to

Indian Institute of Science Education and Research Pune

in partial fulfilment of the requirements for the

BS-MS Dual Degree Programme

by

Goutham Sukumaran

20141148



Indian Institute of Science Education and Research Pune

Dr. Homi Bhabha Road,

Pashan, Pune 411008, India.

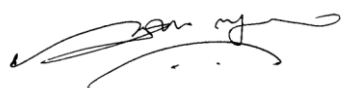
April 2019

Supervisor: Dr. Partha Hazra

Associate Professor, IISER Pune

# Certificate

This is to certify that this dissertation entitled “Exploring Halloysite Nanotube and Halloysite Nanotube- Graphene Oxide Composite Material as Carriers of Anti-cancer Drugs” towards the partial fulfilment of the BS-MS dual degree programme at Indian Institute of Science Education and Research, Pune represents work carried out by Goutham Sukumaran at Indian Institute of Science Education and Research, Pune under the supervision of Dr. Partha Hazra, Associate Professor, Department of Chemistry, during the academic year 2018-2019.



Signature of Student



Signature of Supervisor

Place: Pune

Date: 20.03.2019

# Declaration

I hereby declare that the matter embodied in the report entitled “Exploring Halloysite Nanotube and Halloysite Nanotube-Graphene Oxide Composite Material as Carriers for Anti-cancer Drugs” are the results of the work carried out by me at the Department of Chemistry, Indian Institute of Science Education and Research, Pune, under the supervision of Dr. Partha Hazra and has not been submitted elsewhere for any other degree.



Signature of Student



Signature of Supervisor

Place: Pune

Date: 20.03.2019

## Acknowledgements

First of all I am deeply thankful to my thesis supervisor Dr. Partha Hazra for giving me the opportunity to work under him. His unending help and valuable suggestions led to successful completion of my project. I would also like to thank my TAC member Dr. Angshuman Nag for his continuous support. I am very much thankful to my lab members, Dr. Raj Kumar Koninti, Mr. Sagar Satpathi, Ms. Konoya Das, Mr. Aslam Uddin, Mr. Joy Chatterjee, Mr. Abhijit Chatterjee, Mr. Bibhisan Roy and Dr. Imtiyaz Bhatt. They have guided me in every steps of my project tenure. It would have been impossible to finish my work without their continuous support. I want to thank Mr. Plawan Kumar Jha from Dr. Nirmalya Ballav's Group, Mr. Bharat Tandon and Mr. Vikash Kumar Ravi from Dr. Angshuman Nag's Group, Mr. Partha Samanta and Mr. Subhajit Dutta from Dr. Sujit K. Ghosh's group for their guidance and help. I also express my gratitude to Prof. Jayant B. Udgaonkar, Director, IISER Pune for providing excellent research equipments in the institute. I am grateful to all the technical and non-technical staffs of the department.

. I also want to thank all my friends, especially Sruthy and Namithasree. You have motivated me, guided me and have always been there for me. Thank you so much for all the memories! I am also grateful to my parents and my sister for all the support and love.

.

## Contents

1. Introduction.....	8
2. Methods.....	10
3.1 Loading an Anti-Cancer Drug Ellipticine onto Halloysite Nanotubes and Its Subsequent Release to DNA.....	12
3.2 Loading of Doxorubicin onto Halloysite Nanotubes and Exploration of Dual Drug Loading onto DOX loaded HNT.....	20
3.3 Formation of Composite Material between HNT and GO and Its Application towards Dual Drug Loading.....	32
4. Conclusion.....	41
Future Directions.....	43
References.....	44

## List of Figures

1. Fig. 1 Emission spectra of EPT in DCM with gradual addition of HNT ( $\lambda_{\text{ex}} = 350$ nm).....	13
2. Fig. 2 Normalised emission spectra of (a) EPT in DCM, EPT-HNT in DCM, EPT in buffer, EPT-HNT in buffer (b) EPT in buffer, EPT-HNT dispersed in buffer and HNT added EPT in buffer ( $\lambda_{\text{ex}} = 350$ nm).....	14
3. Fig. 3 Images of (a) HNT and (b) EPT loaded HNT.....	14
4. Fig. 4 Confocal Microscopy images of (a) HNT and (b) EPT-HNT.....	15
5. Fig. 5 (a) Nitrogen adsorption-desorption isotherms and (b) pore size distribution of HNT and EPT-HNT.....	16
6. Fig. 6 Emission spectra of EPT-HNT with progressive addition of ct-DNA ( $\lambda_{\text{ex}} = 350$ nm).....	17
7. Fig. 7 Circular Dichroism spectra of ct-DNA with progressive addition of EPT-HNT.....	17
8. Fig. 8 Fluorescence lifetime transients of EPT in DCM, EPT in buffer, EPT-HNT in DCM, EPT-HNT in buffer and EPT-HNT with ct-DNA.....	18
9. Fig. 9 Images of (a) HNT and (b) DOX loaded HNT.....	22
10. Fig. 10 Emission spectra of (a) DOX and supernatant after DOX loading in HNT, (b) DOX and DOX-HNT in buffer ( $\lambda_{\text{ex}} = 470$ nm).....	23
11. Fig. 11 (a) Emission spectra ( $\lambda_{\text{ex}} = 470$ nm) and (b) excitation spectra ( $\lambda_{\text{em}} = 590$ nm) of DOX with HNT addition.....	23
12. Fig. 12. Stern-Volmer plot of DOX-HNT.....	24
13. Fig. 13. TEM images of (a,b) HNT and (c,d) DOX-HNT.....	25
14. Fig. 14. Pore size distribution of HNT and DOX-HNT.....	26
15. Fig. 15. Fluorescence lifetime transients of DOX with gradual addition of HNT.....	27
16. Fig. 16. Emission spectra of EPT with gradual addition of DOX-HNT in (a) DCM and (b) buffer ( $\lambda_{\text{ex}} = 350$ nm).....	29
17. Fig. 17. Emission spectra of EPT with (a) gradual addition of treated-HNT in DCM and (b) with gradual addition of DOX in buffer ( $\lambda_{\text{ex}} = 350$ nm).....	29
18. Fig. 18. FT-IR spectra of HNT and HNT-NH <sub>2</sub> .....	35
19. Fig. 19. FE-SEM images of (a) HNT, (b) GO and (c,d) HNT-GO.....	36

20. Fig. 20. TGA thermograms of GO, HNT and HNT-GO.....	37
21. Fig. 21. FT-IR spectra of HNT-NH <sub>2</sub> , GO and HNT-GO.....	37
22. Fig. 22. Emission spectra of EPT with gradual addition of (a) GO and (b) HNT-GO ( $\lambda_{ex} = 350$ nm).....	38
23. Fig. 23. Emission spectra of DOX with gradual addition of HNT-GO ( $\lambda_{ex} = 470$ nm).....	39
24. Fig. 24: Emission spectra of (a) EPT-HNT-GO system with addition of DOX ( $\lambda_{ex} = 350$ nm) and (b) DOX before and after addition of EPT-HNT-GO system ( $\lambda_{ex} = 470$ nm).....	39

### List of Tables

1. Table 1. Zeta potential values of HNT and EPT-HNT.....	15
2. Table 2. Fluorescence lifetime fittings of EPT in DCM, EPT in buffer, EPT-HNT in DCM, EPT-HNT in buffer and EPT-HNT with ct-DNA.....	18
3. Table 3. Stern-Volmer quenching constant and biomolecular quenching rate constant.....	25
4. Table 4. Zeta potential values of HNT and DOX-HNT.....	26
5. Table 5. Fluorescence lifetime fittings of DOX in buffer with gradual addition of HNT.....	27
6. Table 6. Porous structural data and zeta potential of HNT and HNT-NH <sub>2</sub> .....	36

## Abstract

Halloysite nanotube (HNT) has many advantages over most inorganic drug delivery systems, like, carbon nanotubes and graphene oxide due to its abundance in nature, low cost and biocompatibility. Most importantly, difference in inside/outside chemistry probably makes HNT as a suitable and unique dual drug delivery carrier. In this project, I have explored HNT as a drug carrier for two anticancer drugs: Ellipticine (EPT) and Doxorubicin (DOX).

In section 3.1, EPT loading to HNT surface has been achieved and it was found that cationic EPT molecules attach to the negative external surface of HNT. In presence of DNA, the loaded EPT was found to release and bind to DNA.

In the next section (3.2), loading of another well-known anticancer drug DOX to HNT was achieved, where the drug molecules mainly occupy the inner lumen. After confirmation that DOX mainly loaded inner lumen, the possibility of loading EPT onto DOX loaded HNT was explored. However, steady-state fluorescence studies suggests the existence of interaction between the loaded EPT and DOX molecules, which are not desirable in a drug carrier, since it may lead to many complications.

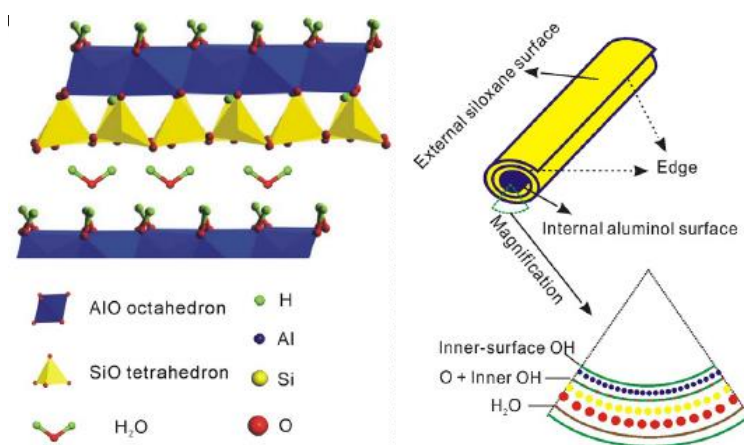
In section 3.3, to obtain a dual drug carrier, a composite material of HNT and graphene oxide (GO), i.e. (HNT-GO) was synthesised and was characterised through various techniques such as FT-IR, FE-SEM and TGA. Steady-state studies confirmed the loading of both the drugs simultaneously onto the material and more importantly, no indication of interactions between EPT and DOX molecules were observed. Therefore, the absence of interactions between the drug molecules makes the composite material (HNT-GO), a suitable choice for the dual delivery carrier of both DOX and EPT.



## 1. Introduction

Targeted drug delivery and sustained release are one of the major concerns in chemotherapy of cancer. Anticancer drugs are often poorly soluble in water and exhibit low selectivity to tumor cells against normal cells, causing severe toxicity to the latter.<sup>1</sup> These factors hampers the widespread application of chemotherapy. One possibility to overcome these limitations is by loading the anticancer drugs to drug delivery systems to achieve targeted delivery and sustained release. Many nanoparticles like carbon nanotubes, graphene oxide, mesoporous silica nanoparticles, micelles, polymer and liposomes has been explored as carriers for drug delivery.<sup>1</sup> However, high cost and toxicity of most of such materials hinders their large-scale applications. Hence, considerable efforts have been invested to obtain cheap, biocompatible nanomaterials for drug delivery applications.

Halloysite (HNT) is a naturally occurring clay mineral with the stoichiometry of  $\text{Al}_2\text{Si}_2\text{O}_5(\text{OH})_4 \cdot n\text{H}_2\text{O}$  where  $n$  is the intercalated water.<sup>2</sup> HNT has a cylindrical structure, consisting of rolled aluminosilicate layers with external diameter of 40-60 nm, internal diameter of 10-15 nm and length of 700-1000 nm.<sup>2</sup> The Halloysite tube wall consists of corner-shared tetrahedral  $\text{SiO}_4$  sheet stacked with an edge-shared octahedral  $\text{AlO}_6$  sheet with an internal aluminol group  $\text{Al-OH}$  (**Scheme 1**).<sup>3</sup> The aluminosilicate sheets are rolled up into a tube such that the siloxane surface forms the external surface with the aluminol groups in the inner lumen encapsulating water in between the layers.<sup>2</sup> Small number of aluminol and silanol groups are also found at.



surface defects of HNT.<sup>4</sup> The different chemical composition and properties of the internal and external surface leads to the different surface charges for the inner and outer layers of HNT. The siloxane outer surface of HNT is negatively charged above pH 1.5 whereas the internal alumina lumen is positively charged below pH 8.5. The material exhibits an overall negative zeta potential of around -30 mV in the pH range 4 to 8.<sup>2</sup>

The morphology, size and the charge distribution of HNT makes it an ideal choice for loading various macromolecules like drugs,<sup>3</sup> biocides,<sup>3</sup> DNA<sup>5</sup> and proteins<sup>6</sup>. The difference in surface charge of inner lumen and outer surface enables neutral and anionic molecules to be encapsulated into the inner lumen whereas cationic molecules can be attached to the negatively charged external surface. The loading can be achieved either by covalently attaching the molecule to HNT surface or via non-covalent interactions. The release time for the loaded agents were also found to be considerably delayed, thus providing sustained release.<sup>3, 7</sup> Cellular uptake and toxicity studies of HNT has found the clay to be non-toxic and biocompatible.<sup>8</sup> Apart from loading molecules onto pristine HNT, the HNT surfaces, due to their different physical and chemical properties, can be functionalised easily to achieve selective adsorption and stimuli responsive release.<sup>9, 10</sup> Moreover, the applications of HNT is not limited to drug delivery systems. Morphology, high surface area and the charge distribution enables Halloysite to be a good adsorbent of both cationic and anionic impurities. Therefore, HNT has been used for water purification systems and the empty inner lumen can also be used as a template for catalytic nanoparticles.<sup>11</sup>

HNT has advantage over most inorganic drug delivery systems like carbon nanotubes and graphene oxide due to its abundance in nature, low cost and biocompatibility.<sup>2</sup> Possibility of easy functionalization also enables synthesis of various composite materials with enhanced properties. The difference of inside/outside chemistry also indicates the possibility of achieving dual drug loading as well. In this project, I have explored HNT as a drug carrier for two anticancer drugs: Ellipticine and Doxorubicin. The possibility of attaining dual drug loading in HNT was also explored in this work. However, indications of interactions between the drug molecules, makes pristine HNT not suitable for dual drug loading of DOX and EPT. Therefore, in section 3.3, composite material of HNT with Graphene Oxide and the prospect of attaining dual drug loading of DOX and EPT in the composite material was investigated.

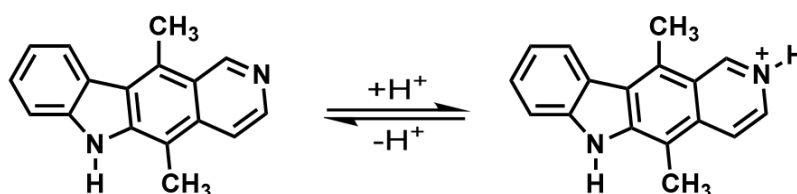
## 2. Methods

All absorption measurements were obtained using Shimadzu UV-Visible spectrometer (Japan) and fluorescence measurements using Fluoromax-4 (HORIBA scientific, USA). Time resolved fluorescence measurements were performed using a time correlated single photon counting (TCSPC) spectrometer (Horiba Jobin Yvon IBH, U.K) with excitation by 375 nm and 405 nm nano-LED in the case of Ellipticine and Doxorubicin respectively, for exciting the drug molecules. Analysis of emission decays were performed using IBH DAS6 analysis software and the lifetime data was fitted with minimum number of exponentials. Best fit was determined by examining  $\chi^2$  values and visually inspecting the residuals.  $\chi^2 \approx 1$  was deemed to be the best fit for the decays. All steady state and time resolved measurements were done at room temperature ( $298 \pm 1$  K). Circular Dichroism (CD) spectra were obtained using J-815 CD (JASCO, USA). Pore size, volume and surface area were determined from N<sub>2</sub> adsorption-desorption isotherms obtained at 77 K on BelSorpmax (Bel Japan) apparatus. Prior to adsorption measurements, the sample was heated at 100°C for 24 hours. Brunauer-Emmett-Teller (BET) method was used to obtain specific surface area and Barrett-Joyner-Halenda (BJH) method was utilised to get pore size distribution of the sample. Zeta potential measurements were performed using Nano-ZS90 Zetasizer instrument (Malvern Panalytical, UK). Zeta potential measurements were made in dispersions in Millipore water with sample concentration of 1 mg/ml. For confocal microscopy imaging, dispersions were made in buffer and dried in vacuum and the images were obtained using Leica confocal laser scanning microscope. ImageJ software was used for evaluating confocal images. Field-emission Scanning Electron Microscopy (FE-SEM) images were obtained using Zeiss Ultra Plus analytical FE-SEM (Zeiss, Germany). FE-SEM samples were prepared in Millipore and was casted onto silicon wafer and dried under vacuum at room temperature overnight. Gold coating was applied to FESEM sample surface to inhibit charging and thermal damage during measurements. High-Resolution Transmission Electron Microscopy (HRTEM) images were captured using UHR FEG-TEM, JEOL JEM 2100F field emission transmission electron microscope operated at an accelerating voltage of 200 kV. A drop of sample prepared in Millipore water was placed onto copper grids and dried in vacuum for TEM imaging. Fourier-transform infrared (FT-IR) spectroscopy was

performed in Thermo Scientific Nicolet 6700 spectrophotometer. Sample containing KBr pellets were prepared for obtaining IR spectra and the data was collected from  $4000\text{ cm}^{-1}$  to  $400\text{ cm}^{-1}$ . Thermogravimetric analysis (TGA) was obtained using Perkin-Elmer STA 6000 TGA analyser under  $\text{N}_2$  atmosphere with a rate of  $10^\circ\text{C min}^{-1}$ . Specific descriptions of materials and methods used are provided in the respective chapters.

### 3.1. Loading an Anti-Cancer Drug Ellipticine onto Halloysite Nanotubes and Its Subsequent Release to DNA

Ellipticine (5,11-dimethyl-6*H*-pyrido [4,3-*b*] carbazole) is a naturally occurring plant alkaloid and it exhibits antitumor and anti-HIV activity.<sup>12</sup> Ellipticine (EPT) achieves antitumor activity by intercalating in DNA and inhibiting the activity of DNA topoisomerase-II, which restricts the process of DNA replication.<sup>13</sup> Due to its biological importance, the optical properties of EPT has also been extensively investigated. Fluorescence of EPT is highly dependent on polarity and pH of the medium. EPT exists in two forms: the neutral form and the protonated form (by protonation of pyridine nitrogen, which has pK<sub>a</sub> value of 7.4) (**Scheme 2**).<sup>14</sup> In non-polar and polar aprotic solvents, EPT exists in its neutral form which emits at blue region (around 410-440 nm), whereas protonated form exclusively exists in aqueous medium and emits green colour at ~530 nm.<sup>15</sup> Poor solubility in aqueous medium and high toxicity hinders the pharmaceutical application of EPT. One strategy to overcome these limitations is by achieving targeted delivery and sustained release. Therefore, various nanomaterials like mesoporous silica nanoparticles,<sup>16</sup> graphene oxide,<sup>17</sup> micelle,<sup>18</sup> reverse micelle<sup>19</sup> and cyclodextrin<sup>20</sup> has been explored as carriers for the targeted delivery of EPT. As mentioned earlier, high abundance and biocompatibility distinguishes Halloysite from other drug delivery systems. In this study, I have explored Halloysite as a potential carrier of EPT. The EPT loaded HNT was characterised through various techniques and interaction of the EPT loaded HNT with biomolecules was also investigated.



**Scheme 2.** Different prototropic forms of ellipticine.

#### Experimental Section

Halloysite nanotube (HNT) and calf thymus DNA sodium salt (ct-DNA) were purchased from Sigma-Aldrich, and Ellipticine (EPT) was purchased from Cayman Chemicals. All the chemicals were used without further purification. Molecular biology

grade potassium phosphate monobasic and sodium phosphate dibasic were obtained from Sisco Research Laboratories (SRL India) and used for the preparation of 10 mM Phosphate buffer of pH 7. Halloysite nanotubes were dried in oven at 150 °C to remove the trace amount of encapsulated water molecules. EPT stock solution was prepared in dimethyl sulfoxide (DMSO) solvent. Drug loading was achieved by adding thermally activated HNT to EPT in dichloromethane (DCM). EPT loaded HNT (EPT-HNT) was washed several times with DCM to remove unbound or weakly bound drug molecules. The supernatant emission spectra does not have any peaks corresponding to neutral form of EPT and it is identical to the emission of pure DCM solvent. This confirms that EPT is attached to the HNT. EPT-HNT was dried overnight and extracted from DCM. EPT-HNT was then dispersed onto 10mM pH 7 phosphate buffer. ct-DNA sample was annealed at 90-95°C and gradually cooled to room temperature. The concentration of calf thymus DNA was estimated by the absorbance at 260 nm using extinction coefficient of 6600 M<sup>-1</sup> cm<sup>-1</sup>.

## Results and Discussion

### Steady-State Fluorescence and Circular Dichroism Measurements

Ellipticine in DCM exhibits an emission maxima ~425 nm, which corresponds to the

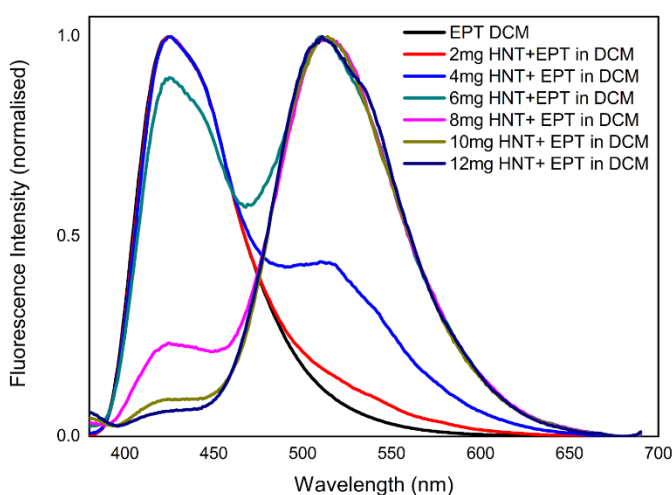


**Fig 1.** Emission spectra of EPT in DCM (3ml) with gradual addition of HNT ( $\lambda_{\text{ex}} = 350$  nm).

neutral form of the molecule.<sup>15</sup>

However, with the gradual addition of the HNT, the 425 nm peak is getting diminished and a new peak at 510 nm arises progressively (**Fig. 1**).

This new peak can be attributed to the protonated form of EPT.<sup>15</sup>

Hence, we can infer that the neutral form of EPT is getting converted to the protonated form in presence of HNT, and the switching from neutral to protonated form is completed

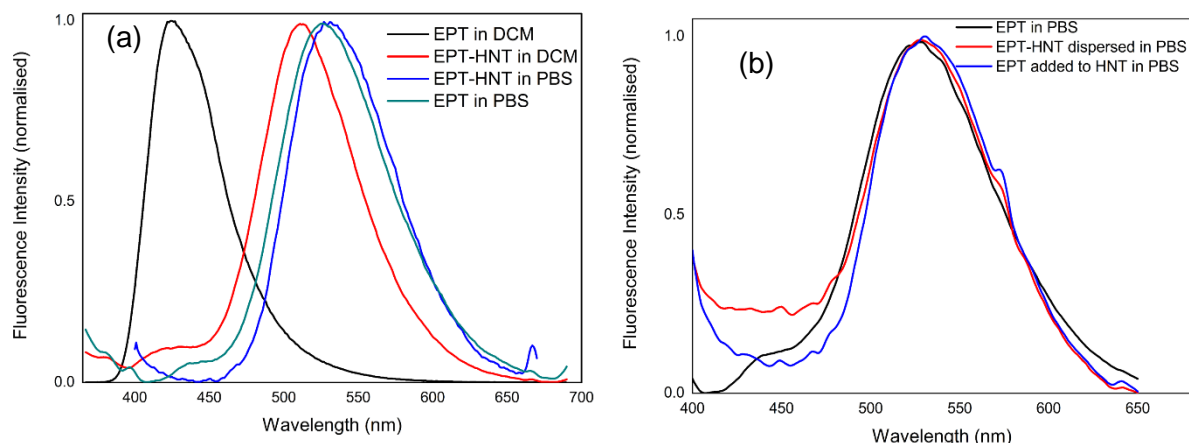


**Fig 2.** Normalised emission spectra of (a) EPT in DCM and PBS with and without HNT and (b) EPT-HNT extracted from DCM and dispersed in buffer and HNT added EPT in buffer.

upon addition of 12 mg HNT in 3 ml DCM. This switching confirms the loading of the drug on/into HNT. The switching can be attributed to the protonation of EPT by -Si-OH groups present on HNT surface. Notably,  $pK_a$  -Si-OH group is around 5<sup>21</sup> and the  $pK_a$  of EPT is 7.4,<sup>14</sup> thus it is expected that EPT can abstract the proton from silanol group, when EPT binds to HNT, and the protonated EPT can then electrostatically interact with the negatively charged HNT surface. The drug loaded Halloysite was then extracted and dispersed in phosphate buffer of pH=7. The emission spectra of EPT loaded HNT shows a single peak around 532 nm. The peak value is more or less the same as that of EPT in buffer, which also has a peak ~530 nm (**Fig 2**). The lack of shift in peak position of EPT-HNT in buffer when compared to EPT in buffer suggests that in both the cases, molecule is exposed to similar polarity conditions. Since the polarity of outside surface is closed to the polarity of the bulk medium, we can conclude that the cationic EPT molecules are attached to the negatively charged external surface of HNT.

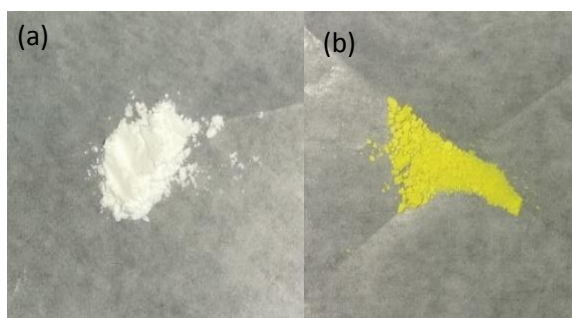


**Fig 3.** HNT before (a) and after (b) EPT loading.

Drug loading was confirmed by various other characterisation methods. Most obvious confirmation of drug loading in HNT is the colour change: white coloured HNT turns to bright yellow upon EPT loading (**Fig. 3**). EPT loading on HNT was also confirmed by confocal microscopy (**Fig. 4**). HNT by itself does not

show any fluorescence, hence does not give any signal in confocal imaging. However, due to the presence of EPT, drug loaded HNT is fluorescent and can be visualised through confocal imaging. The green particles in the confocal image of EPT-HNT

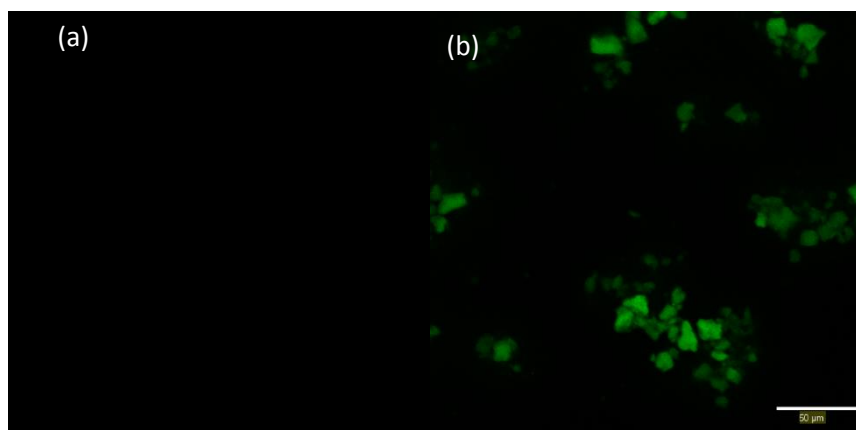


**Fig 4.** Confocal images of HNT before (a) and after (b) EPT loading.

**Table 1:** Zeta potential values of HNT and EPT-HNT.

Sample	Zeta potential (mV)
HNT	$-34.54 \pm 2.45$
EPT-HNT	$-8.45 \pm 2.91$

indicate that the EPT molecules are attached to HNT. HNT and EPT loaded HNT were characterised through zeta potential measurements, which can provide insights about the surface charge of the particles (**Table 1**). The zeta potential of HNT was found to be around -34 mV and was in accordance with literature reports.<sup>3</sup> However, upon drug loading the value of surface charge was observed to decrease from - 34 to around -8 mV. The shift in the value suggests that the cationic drug molecule is attached to the negatively charged external surface, thereby, reduces the surface charge of the system. Therefore, zeta potential measurement also supports that the drug is loaded onto the external surface.

Gas adsorption-desorption isotherms of HNT and EPT-HNT were also utilised to understand the loading and the structural parameters. The nitrogen adsorption-



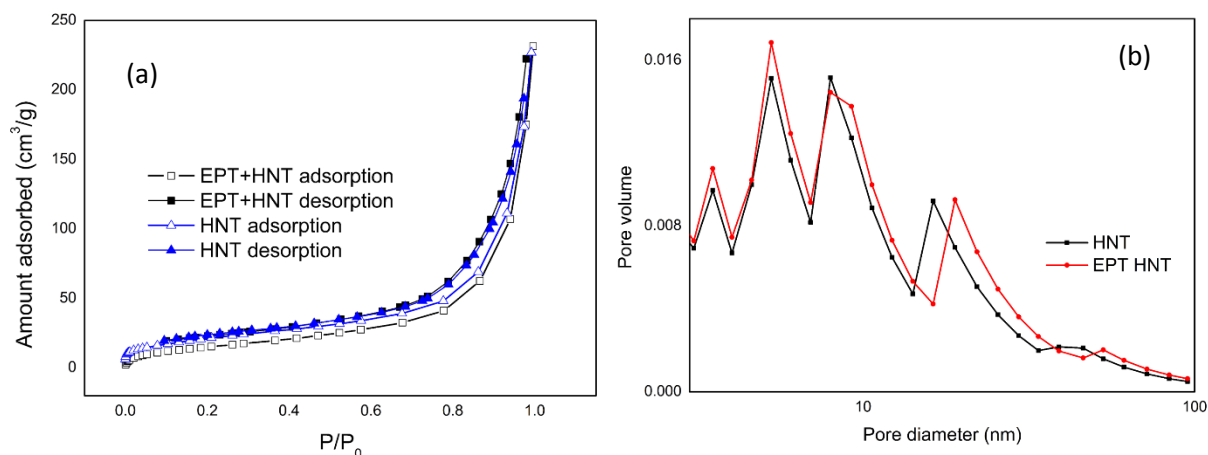


**Fig 5.** (a) Nitrogen adsorption-desorption isotherms and (b) pore size distributions of HNT and EPT-HNT.

desorption isotherm for HNT and EPT-HNT can be classified as type II with H3 hysteresis loop, characteristic of macroporous and mesoporous materials and is consistent with earlier reports (**Fig. 5a**).<sup>22</sup> The pore size distribution of HNT and EPT-HNT were also obtained through Barrett-Joyner-Halenda (BJH)<sup>23</sup> analysis of the isotherms (**Fig. 5b**). Three peaks appear prominently in the distribution, around 5 nm, 8 nm and 16 nm. The 5 nm peak has been attributed to the newly formed pores upon dehydration of HNT and structural defects by Yuan *et al.*<sup>24</sup> The remaining peaks of diameter 8 and 16 nm can be assigned to inner lumen of HNT. The diameter of pores were found to be almost identical in both HNT and EPT-HNT, as well as the pore volume, suggesting that the inner lumen is not blocked or obstructed upon drug loading. This observation also supports that the drug is being loaded onto the external surface, not in the inner lumen of HNT.

For application as a drug carrier, it is important to investigate the interaction between EPT loaded HNT and various biomolecules. Since the EPT achieves antitumor activity by intercalating with DNA, interaction of EPT-HNT with DNA was explored in this study. Fluorescence intensity of EPT was found to gradually increase with progressive addition of ct-DNA without any significant shift in the peak maxima (**Fig. 6**). The observation is in accordance with results from earlier studies of EPT-DNA interactions, suggesting that the drug molecules are being released from HNT in presence of DNA.<sup>16</sup> The interaction between DNA and EPT-HNT was also explored through circular dichroism (CD) studies. CD spectrum of ct-DNA in phosphate buffer

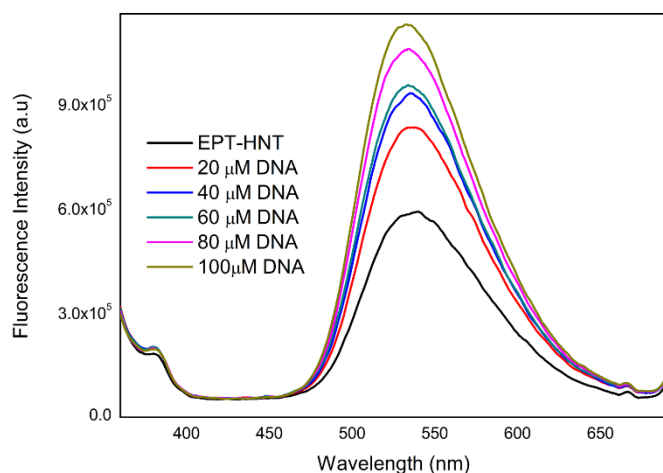


**Fig 6.** Emission spectra of EPT-HNT in buffer with progressive addition of ct-DNA ( $\lambda_{ex} = 350\text{nm}$ ).

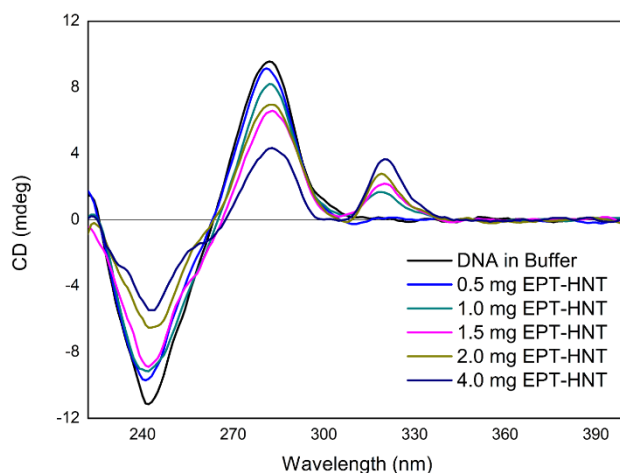


**Fig 7.** CD spectra of ct-DNA in buffer with progressive addition of EPT-HNT.

has two peaks: a positive peak around 280 nm and a negative peak around 245 nm (**Fig. 7**). With progressive addition of EPT loaded HNT, the bands at 280 and 245 nm are getting diminished, while a new positive band appears around 320 nm. This profile is identical to CD spectra of EPT-DNA system in which EPT intercalation with DNA gives rise to induced CD band near 320 nm.<sup>16</sup> Therefore, CD measurements also suggests that EPT is getting released from HNT in presence DNA followed by intercalation in DNA, possibly due to the higher binding affinity of EPT towards DNA.

## Time-resolved Fluorescence Results

Fluorescence lifetime measurement can provide better insight about excited state environment. Thus, lifetime measurement was utilised to explore the interaction of EPT with HNT and EPT-HNT with DNA (**Fig. 8**). EPT in DCM shows biexponential decay with average lifetime of 14.4 ns (**Table 2**). Major contribution in the decay comes from the long lifetime component of 16.6 ns. This value is in agreement with previous studies in which EPT was found to have long lifetime component in nonpolar solvents.<sup>15</sup> Therefore, the long lifetime component can be assigned to neutral form of EPT. EPT in buffer has an average lifetime of 2.4 ns with a biexponential decay profile. Major contribution comes from 1.91 ns component, which can be assigned to the protonated of EPT in aqueous media.<sup>25</sup> When HNT is added to EPT in DCM, the

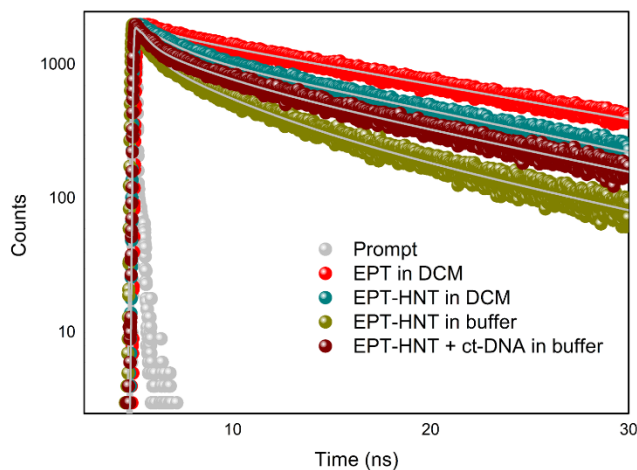


**Fig 8.** Fluorescence transients ( $\lambda_{\text{ex}} = 375 \text{ nm}$ ) of EPT in DCM ( $\lambda_{\text{col}} = 430 \text{ nm}$ ), EPT-HNT in DCM ( $\lambda_{\text{col}} = 510 \text{ nm}$ ), EPT-HNT in buffer ( $\lambda_{\text{col}} = 530 \text{ nm}$ ) and EPT-HNT with ct-DNA addition ( $\lambda_{\text{col}} = 530 \text{ nm}$ ).

average lifetime is reduced to 8.9 ns with the decay exhibiting tri-exponential feature. EPT-HNT when dispersed in buffer shows an average lifetime of 4.4 ns. Although it is difficult to assign each component individually, the significant increase in average lifetime from 2.4 ns in case of EPT in buffer to 4.4 ns when EPT-HNT is dispersed in buffer implies the presence of strong interaction between EPT and HNT. The average lifetime was found to further increase

to 6.68 ns when DNA was added to the system. The contribution from long lifetime component was found to increase from 21% to 41% with addition of ct-DNA. The appearance of the long lifetime component of around 16 ns was previously reported in DNA-EPT system and was attributed to the intercalation of EPT to DNA.<sup>25</sup> Therefore presence of long lifetime component in EPT-HNT system with the addition of DNA also suggests that EPT is getting released from HNT and intercalating in between DNA base pairs.

**Table 2.** Fluorescence lifetime fittings of EPT in different conditions collected at their respective emission maxima ( $\lambda_{\text{ex}} = 375 \text{ nm}$ ).

Sample	$\alpha_1$	$\tau_1 \text{ (ns)}$	$\alpha_2$	$\tau_2 \text{ (ns)}$	$\alpha_3$	$\tau_3 \text{ (ns)}$	$\tau_{\text{av}} \text{ (ns)}$	$\chi^2$
EPT in DCM	0.15	1.72	0.85	16.64	—	—	14.4	1.01
EPT-HNT in DCM	0.22	3.52	0.53	14.83	0.25	0.79	8.94	0.95
EPT-HNT in buffer	0.31	3.96	0.21	13.59	0.48	0.62	4.38	0.97
EPT in buffer	0.13	5.74	—	—	0.87	1.91	2.41	1.08
EPT-HNT+ DNA	0.23	3.35	0.41	14	0.36	0.52	6.68	1.02

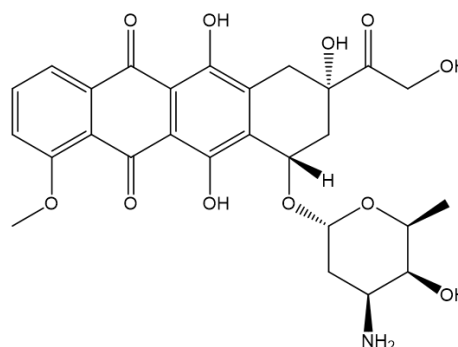
## Conclusion

The anticancer drug Ellipticine was successfully loaded onto Halloysite nanotubes. The loading was confirmed through fluorescence switching of EPT molecules in DCM solvent since the blue emission (corresponding to the neutral form of the drug) switches to green emission (coming from the protonated form) in presence of HNT. The existence -Si-OH groups, which can donate proton is assumed to facilitate the conversion of neutral form of EPT to the protonated form when getting loaded onto HNT. From the absence of any shift in the emission peaks of EPT-HNT when compared to that of EPT in buffer, indicate that the drug is attached to the negatively charged external surface, possibly through electrostatic interactions. The drug loading was also confirmed through various characterisation techniques such as confocal microscopy, zeta potential measurement and gas adsorption-desorption study. Fluorescence lifetime data also confirms strong interaction between EPT and HNT. Furthermore, interaction between EPT-HNT and DNA was also studied through steady-state, lifetime and circular dichroism spectra. The green emission of EPT-HNT was found to increase in intensity with the addition of DNA, signifying that the release of drug from HNT and subsequent binding to DNA. Intercalation of EPT in DNA after being released from HNT was confirmed through appearance of induced CD band and long lifetime component.

### 3.2. Loading of Doxorubicin onto Halloysite Nanotubes and Exploration of Dual Drug Loading in DOX loaded HNT

Monotherapy or the use of a single drug for treatment has its own limitations, like low drug efficacy and development of drug resistance.<sup>26</sup> One approach to overcome these limitations is by combined administration of two or more therapeutic agents, which can provide synergistic effect even at lower drug concentrations.<sup>27</sup> Simultaneous application of drugs having distinct mechanisms of action can also inhibit development of drug resistance and enhance the therapeutic efficacy.<sup>28</sup> Therefore, combination therapy is clearly advantageous over treatment using single drug. Since most of the anticancer drugs require drug carriers to achieve higher efficiency with minimal side effects, identification of carriers which can deliver two distinct drugs simultaneously is a major challenge in combination therapy. In the previous chapter, an anticancer drug Ellipticine was successfully loaded onto Halloysite nanotubes. Here, I am exploring the loading of another anticancer drug Doxorubicin onto HNT and the possibility of achieving dual drug delivery system by loading both Ellipticine and Doxorubicin together to HNT.

Doxorubicin (DOX), commercially known as Adriamycin, is a commonly used chemotherapeutic drug belonging to the category of anthracycline antibiotics, and has been used for the treatment of various cancers including lymphoma, stomach, breast and bladder among several others.<sup>29</sup> DOX molecule consists of a flat anthraquinone linked to an amino sugar, daunosamine through glycosidic bond (**Scheme 3**). The anthraquinone part of the molecule is lipophilic, whereas the daunosamine part is hydrophilic. The solubility of the DOX in water can be enhanced by protonating the amine group of the sugar moiety by forming DOX hydrochloride.<sup>29</sup>



**Scheme 3.** Structure of Doxorubicin.

Anticancer activity of DOX is achieved through the intercalation of the planar anthraquinone moiety into DNA. The intercalation inhibits the progression of topoisomerase II, which is responsible for unwinding of DNA strands for transcription.<sup>30</sup> However, the intercalation of DOX can affect a variety of DNA processes that generate reactive oxygen species, resulting in the decline of mitochondrial oxidative phosphorylation. The attack of reactive oxygen species is believed to be the reason for the cardiotoxicity of DOX.<sup>31</sup> Therefore, the high toxicity and low selectivity towards cancer cells of DOX presents a major hurdle to the application of DOX in cancer treatment. One of the strategies to reduce cardiotoxicity and other undesirable side effects of the drug is by encapsulation in various biocompatible materials. Liposomes, polymer micelles, and nanoparticles has been explored as a possible drug delivery vehicle for DOX.<sup>32, 33</sup>

Halloysite, due to its biocompatibility and morphology is an ideal choice in this context and DOX loading onto HNT has been explored previously. Li *et al.* has investigated the loading of DOX onto HNT.<sup>34</sup> The drug loading was performed in PBS solution of pH 6.5. Since the pKa of the amine group is 8.2<sup>35</sup>, DOX molecules are almost entirely in protonated form in pH 6.5 condition. They have reported that the drug molecules are getting attached to the external surface by electrostatic interactions between the cationic molecule and the negative surface of HNT. However, they have found that some drug molecules were also loaded into the inner lumen as well, and this was attributed to the strong capillary pull which overcomes the repulsion between the positively charged entities.

In this work, I have tried to achieve dual drug loading onto HNT by loading both EPT and DOX simultaneously. From the last chapter, EPT was found to be loaded on the external surface of HNT. In this chapter, I have tried to load DOX mainly on the inner lumen by altering the drug loading conditions such that the lumen filling is facilitated by the DOX. Then, I have explored the possibility of loading EPT onto the DOX loaded HNT (prepared in the above mentioned manner) to achieve dual drug loading.

## Experimental Section

Halloysite nanotubes and doxorubicin hydrochloride were purchased from Sigma-Aldrich and Ellipticine was purchased from Cayman Chemicals. All chemicals were used without further purification. Molecular biology grade potassium phosphate monobasic and sodium phosphate dibasic were obtained from Sisco Research Laboratories (SRL India). Stock solutions of DOX and EPT were prepared in Millipore water and DMSO, respectively.

DOX can exist in cationic, neutral and anionic forms depending on the pH of the medium. The protonation  $pK_a$  of DOX amino group is 8.2 and that for deprotonation of the phenol group is 9.5.<sup>35</sup> The charge separation of internal and external surfaces of HNT does not exist at higher pH (8.5)<sup>36, 37</sup>, also the structure of DOX was found to get destroyed on prolonged exposure to the extreme alkaline environment ( $pH > 9$ ) from our study. Therefore, phosphate buffer (10mM) of pH 8.6 in which most of the DOX molecules exist in the neutral form, was used for loading DOX onto HNT. The drug loading was performed by adding HNT to DOX solution in buffer. Then, HNT-DOX dispersion was also strongly sonicated several times to encourage the release of gas bubbles from inner lumen. After that the solution was stirred for 24 hours at room temperature followed by vacuum cycling for 2 hours to remove the gas bubbles from the lumen for enhancing the drug loading. As a control sample, HNT subjected to the same treatment as that of DOX loaded HNT: sonication, stirring for 24 hours and vacuum cycling in pH 8.6 phosphate buffer. For dual drug loading, DOX loaded HNT (DOX-HNT) extracted from buffer by centrifugation followed by vacuum drying. Then, DOX-HNT powder was added to EPT in dichloromethane (DCM) solvent. The same experiment was also performed in pH 7 10 mM phosphate buffer.



**Fig 9.** (a) HNT (b) DOX loaded HNT.

## Results and Discussion

### Steady-State Fluorescence Measurements

Doxorubicin in buffer exhibits two prominent peaks in the emission spectra: one at around 560 nm and another at 590 nm (**Fig. 10a**). The drug loading was also confirmed by the comparison of emission spectra of DOX in buffer before addition of

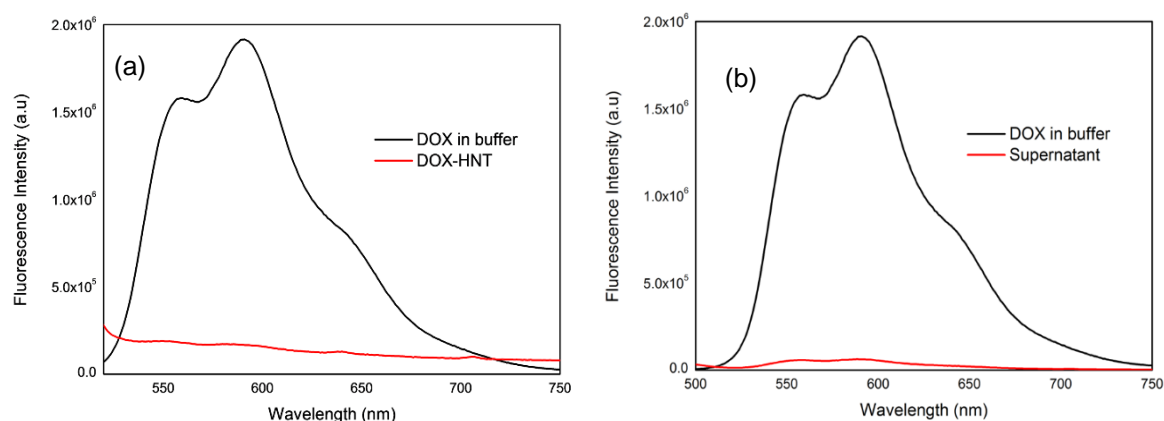


**Fig 10.** Emission spectra of (a) DOX in pH 8.6 buffer and DOX-HNT in buffer and (b) DOX in pH 8.6 buffer and supernatant after removing DOX-HNT ( $\lambda_{ex} = 470$  nm).

HNT and the supernatant of the solution after HNT was added (**Fig. 10b**). Drastically reduced supernatant emission confirms that most of DOX binds to HNT. The most obvious confirmation of drug loading is the colour change of HNT from bright white to pink (**Fig. 9**), when the DOX loaded HNT (DOX-HNT) extracted from buffer by centrifugation followed by vacuum drying.

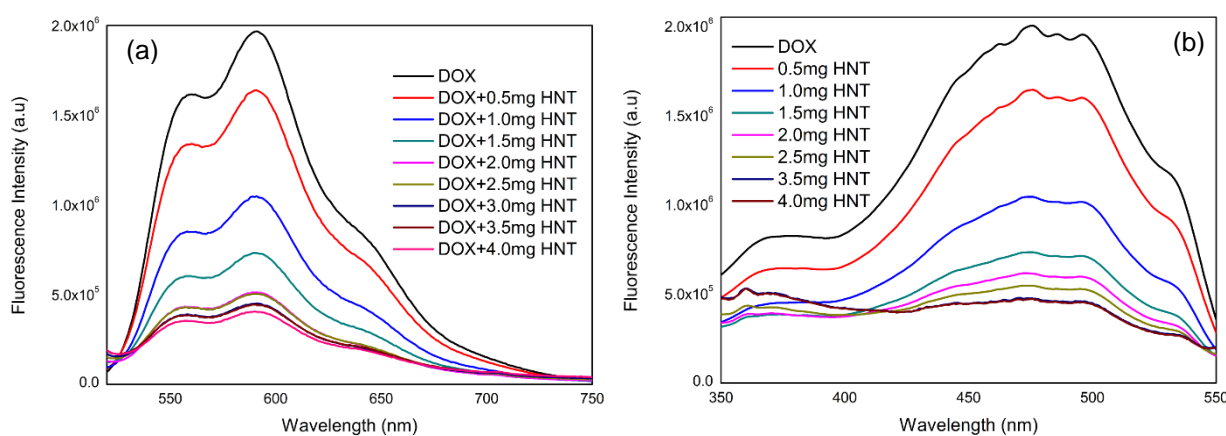


**Fig 11.** (a) Emission spectra ( $\lambda_{ex} = 470$  nm) (b) Excitation spectra ( $\lambda_{em} = 590$  nm) of DOX in pH 8.6 buffer (3 ml) with gradual addition of HNT.



The fluorescence of DOX was found to decrease drastically upon loading onto HNT (**Fig. 10b**). The quenching of DOX emission was confirmed by gradual addition of HNT to DOX solution in buffer (**Fig. 11a**). The intensity of both the 560 nm and 590 nm emission peaks were found to decrease gradually with HNT addition. The trend

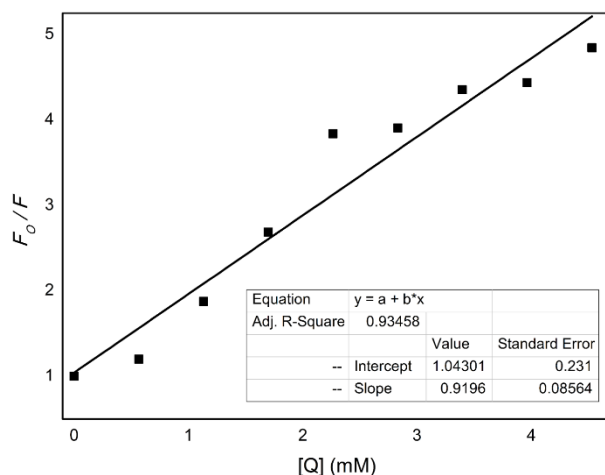


**Fig 12.** Stern-Volmer plot of DOX-HNT.

was also evident even in the excitation spectra of DOX in presence of HNT in which the peak around 480 nm diminishes gradually (**Fig. 11b**). HNT is electron-deficient due to the metal atoms such as aluminium which can accept electron to their empty orbital.<sup>38,</sup>  
<sup>39</sup> Therefore, HNT can involve in electron transfer from electron-rich species. Hence, the quenching of DOX fluorescence likely arises from the

electron transfer from DOX to HNT. From the plot of relative emission intensity with quencher concentration, quenching constant can be calculated using the Stern-Volmer equation:<sup>40</sup>

$$\frac{F_0}{F} = 1 + k_q \tau_0 [Q] = 1 + K_{SV} [Q] \quad (1)$$

where,  $F_0$  and  $F$  corresponds to emission intensities with and without quencher respectively and  $k_q$  is the biomolecular quenching rate constant.  $K_{SV}$ ,  $\tau_0$  and  $[Q]$  are Stern-Volmer quenching constant, fluorescent lifetime of the fluorophore in the absence of quencher and concentration of the quencher respectively (Lakovicz).  $K_{SV}$  is the slope of the linear regression plot of  $F_0 / F$  against  $[Q]$  and  $k_q$  can be calculated by dividing the slope with the lifetime. The values of  $K_{SV}$  and  $k_q$  for DOX-HNT were calculated from the plot (**Fig. 12**) and are provided in **Table 3** ( $\tau_0$  obtained from **Table 5**).

Since the DOX emission is getting quenched, it is not possible to determine whether the drug is loaded onto the inner lumen or external surface solely based on the position of the peaks before and after addition of HNT like in the case of EPT-HNT.

Hence, support from other techniques are required. Therefore, transmission electron microscopy (TEM) of HNT and DOX loaded HNT were utilised to get insight into the

**Table 3.** Stern-Volmer quenching constant and bimolecular quenching rate constant of DOX-HNT system.

$K_{SV}$ (slope) ( $L mol^{-1}$ )	$\tau_0$ (s)	$k_q$ ( $L mol^{-1} s^{-1}$ )
$0.9196 \times 10^3$	$1.01 \times 10^{-9}$	$0.91 \times 10^{12}$

system (**Fig. 13**). The tubular morphology, high aspect ratio and the thick wall with empty inner lumen of HNT can be distinguished from TEM image. In the image of DOX-HNT, the inner lumen can be seen partially filled with some drug molecules (**Fig. 13c**). However, in **Fig. 13d**, the inner and outer surfaces of HNT are observed to be thickened and roughened probably due to the loading of DOX. From the TEM images, we can infer that the drug is being loaded on both the inner lumen and external surface of HNT.

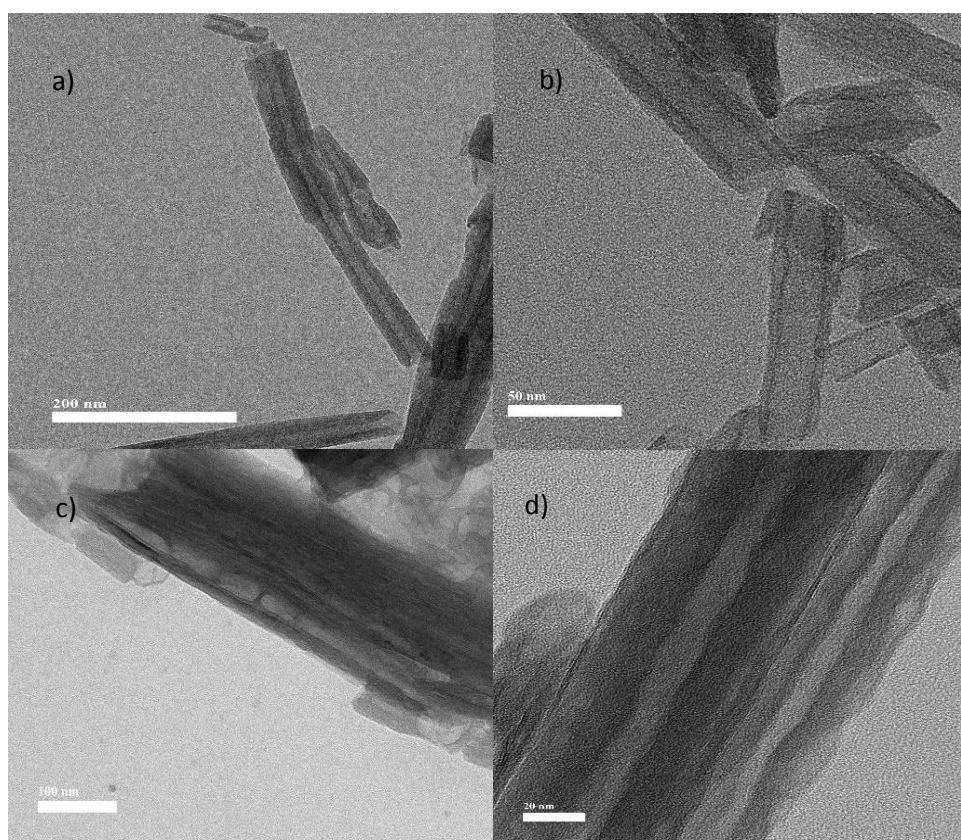


**Fig 13.** TEM images of HNT (a,b) and DOX loaded HNT (c,d).

**Figure 14** depicts the comparison of pore size distributions of HNT and DOX-HNT obtained through BJH analysis<sup>23</sup> of gas adsorption isotherms. Both HNT and DOX-HNT has mainly three peaks. The peaks around 8 nm and 16 nm can be

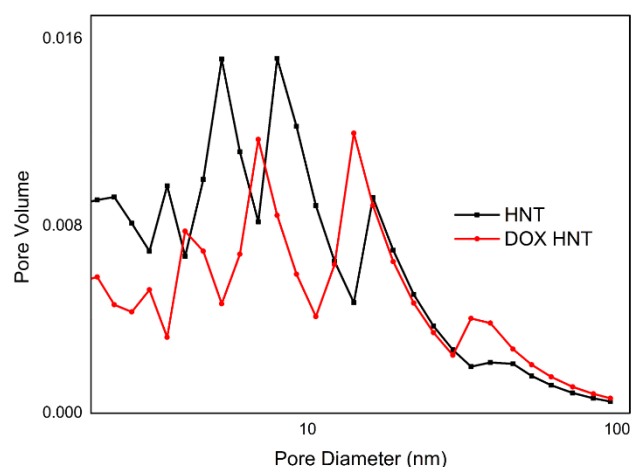


**Fig 14.** Pore size distribution of HNT and DOX-HNT.

attributed to the internal lumens of HNT, whereas the peak at 5 nm can be assigned to the new pores formed during dehydration of HNT and structural defects.<sup>24</sup> All the three peaks were found to have shifted towards lower diameter in the case of DOX-HNT and the lumen peaks have changed from 8 nm and 16 nm to 7 nm and 14 nm, respectively and the pore corresponding to the defects has

shifted from 5 nm to 4 nm. In addition to the shift, the pore volume of the lumen peak has also decreased significantly, suggesting lumen is getting filled by the loaded drug. The 4 nm peak has almost vanished, possibly due to the adsorption of drug molecules on HNT surface. Therefore, the pore size distribution of DOX-HNT confirms the inner lumen loading of DOX molecules. However, the increase in pore volume

corresponding to the 16 nm peak needs to be investigated further.

**Table 4.** Zeta potential values of HNT and DOX-HNT.

Sample	Zeta potential (mV)
HNT	$-34.54 \pm 2.45$
DOX-HNT	$-37.92 \pm 1.87$

Zeta potential measurements of DOX-HNT reveal that the surface charge of HNT remains almost the same even after DOX loading (**Table 4**). If the molecules were loaded onto the external surface, we could have expected a reduction in the negative value of zeta potential due to

masking or neutralisation of the negative surface charge by the molecules. Since the observed zeta potential value does not show any decrement, we can conclude that the molecules are loaded in the inner lumen of HNT. Thus, the slight increase in the negative value of the charge can be attributed to the effect of prolonged exposure of

HNT to basic media (pH 8.5) while the drug loading was carried out. The zeta potential of HNT has already been reported to become more negative with increasing pH, and the prolonged exposure in the basic media can also etch the HNT surface exposing more ionisable hydroxyl groups.<sup>4</sup> Therefore, zeta potential measurements suggests that the DOX molecules are mainly loaded in the inner lumen of HNT.

### Time-resolved Fluorescence Results

Lifetime measurements of DOX in buffer and with progressive addition HNT were collected at 590 nm (**Fig. 15**). DOX in water exhibits monoexponential decay with an average lifetime of 1.01 ns, which is consistent with the literature reports<sup>41</sup> (**Table 5**). With gradual addition of HNT, the decay remained monoexponential and the average lifetimes were also found to remain

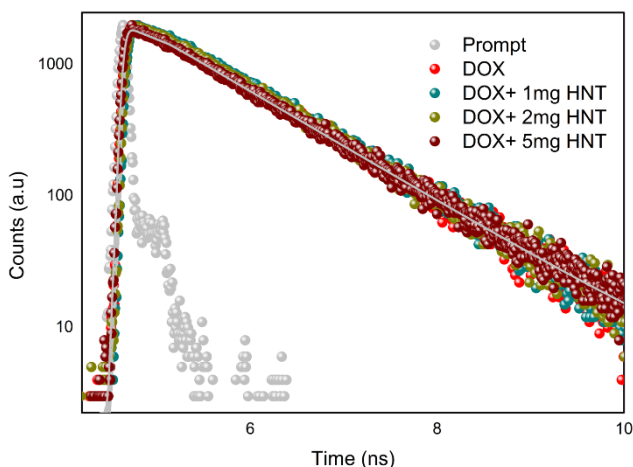


**Fig 15.** Fluorescence transients of DOX in buffer and with addition of HNT ( $\lambda_{ex} = 402$  nm,  $\lambda_{col} = 590$  nm).

constant around 1.01 ns (**Table 5, Fig. 15**). However, the emission intensity gradually decreases with the addition of HNT. Thus, from the lack of changes in fluorescence lifetime of DOX upon HNT addition, we can conclude that the fluorescence quenching mechanism of DOX in presence of HNT is static quenching.

**Table 5.** Fluorescence transient fittings of DOX in buffer with progressive addition of HNT ( $\lambda_{ex} = 402$  nm,  $\lambda_{col} = 590$  nm).

Sample	$\alpha_1$	$\tau_1$ (ns)	$\chi^2$
DOX in buffer	1	1.01	1.006
DOX+ 1 mg HNT	1	1.01	0.996
DOX+ 2 mg HNT	1	1.01	1.07
DOX+ 5 mg HNT	1	1.03	1.09

## Loading Ellipticine to Doxorubicin loaded Halloysite

From the above results, we can conclude that the DOX molecule is being loaded onto both inner lumen and external surface, with the major portion loaded inside the lumen. In the previous chapter, we have seen that the cationic EPT molecule can be loaded onto the negatively charged external surface of HNT. Since the zeta potential of DOX-HNT and HNT does not differ much, the possibility of loading EPT onto the surface of DOX-HNT system was explored in this section.

### Steady-State Fluorescence Measurements

EPT in DCM exists in its neutral form, exhibiting an emission maxima at ~430 nm. With the progressive addition of DOX-HNT, the emission intensity of EPT gradually decreases (**Fig. 16a**). This observation is in stark contrast to the behaviour of EPT when loaded onto HNT alone in DCM (**Fig. 1**). In the case EPT-HNT in DCM, reduction in intensity of 430 nm peak was accompanied by the appearance of a new peak at 510 nm (**Fig. 1**) implying the binding of EPT on HNT surface followed by switching of EPT from neutral to protonated form. However, in the case of DOX-HNT, only quenching of EPT emission was observed, with no switching in emission peak with addition of DOX-HNT. Similar quenching of EPT emission was observed in buffer but with higher efficiency than in DCM (**Fig. 16b**). Thus, the quenching of EPT emission in both DCM and buffer indicates the interaction between the EPT molecule and DOX-HNT. Overall, two important observations from the emission spectra of EPT with DOX-HNT addition in DCM are the absence of switching from neutral to protonated form and the quenching of EPT emission.

In the case of EPT-HNT system, EPT molecules were protonated by the Si-OH groups of HNT surface (as discussed in section 3.1). Since DOX loading onto HNT was carried out at pH 8.6 buffer for extended duration, the effect of such environment on the surface of HNT needs to be taken into consideration. For that HNT powder was subjected conditions similar to that of DOX loading, i.e. stirring at pH 8.6 phosphate buffer along with strong sonication and vacuum cycling. HNT subjected to the treatment was collected by centrifugation followed by drying, and the emission spectra of EPT was monitored with gradual addition of the treated HNT (t-HNT) (**Fig. 17a**). Here, we did not find clear switching from neutral to protonated form, however, there

is a peeping peak of 530 nm at higher amount of t-HNT. Therefore, we can conclude that the switching of EPT from neutral to protonated form was not facilitated in presence of treated-HNT (t-HNT). Possible explanation for this behaviour is that upon alkaline treatment, most of the hydroxyl groups in HNT surface are deprotonated. Hence, EPT molecules, existing in its neutral form, do not find any source to accept protons from when the t-HNT is added. As a result, the switching of EPT from neutral

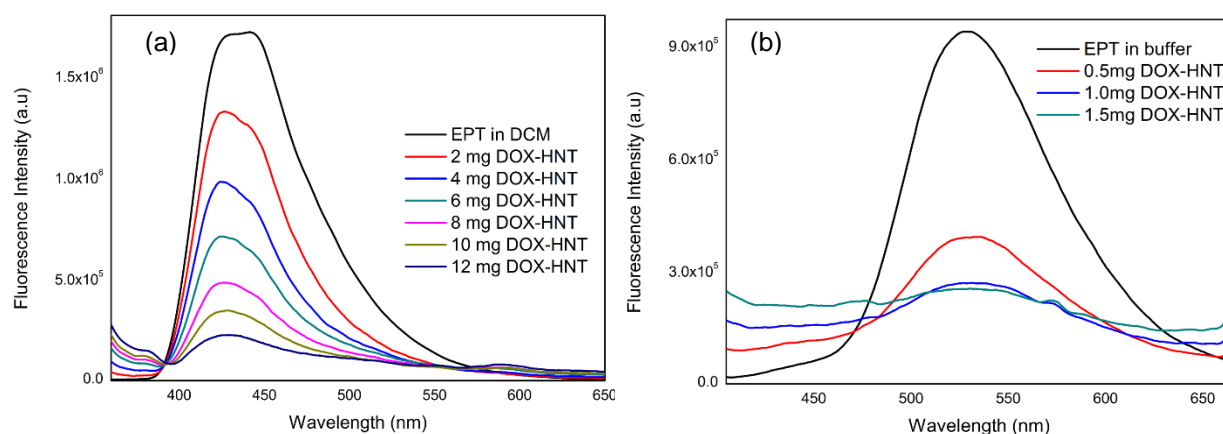


**Fig 16.** Emission spectra of (a) EPT in DCM (3ml) (b) EPT in buffer (3ml) with gradual addition of DOX-HNT ( $\lambda_{\text{ex}} = 350 \text{ nm}$ ).

to protonated form is absent in the case of treated HNT (t-HNT) and in the case of DOX-HNT in DCM (**Fig. 17a**). The slight decrease in the emission intensity of EPT along with an appearance a peeping peak (at 530 nm) with t-HNT addition is likely caused by the switching of a small population of EPT molecules to protonated form by the presence of few hydroxyl groups unaffected by the alkali treatment.

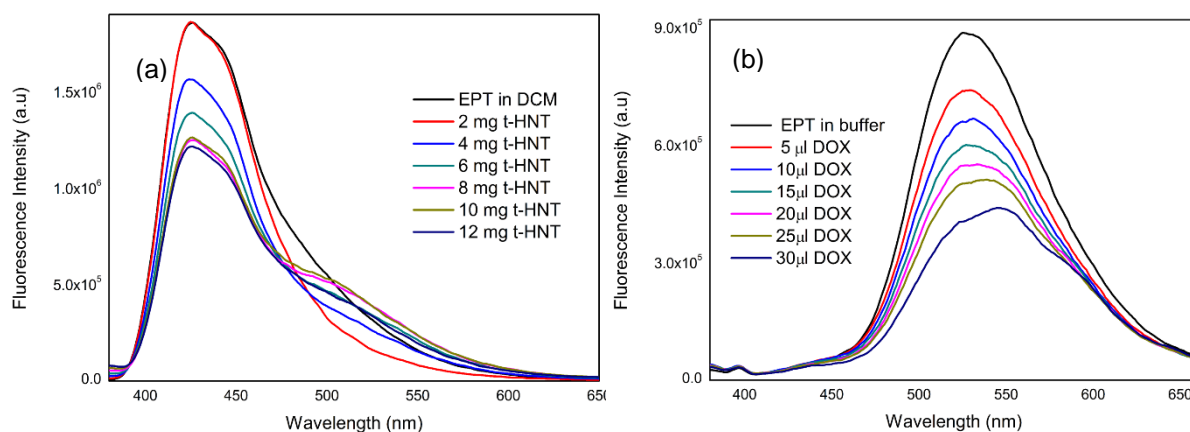


**Fig 17.** Emission spectra of EPT in (a) DCM with gradual addition of treated HNT and (b) phosphate buffer with gradual addition of DOX from 1.1mM stock solution ( $\lambda_{\text{ex}} = 350 \text{ nm}$ ).

Since quenching of EPT emission was not observed when treated-HNT was added to EPT, the quenching of EPT by DOX-HNT is probably caused by the interaction of DOX and EPT molecules present in the outer surface and lumen openings. In order to understand more, emission spectra of EPT was monitored with gradual addition of DOX in the absence of HNT (**Fig. 17b**). Due to the low solubility of DOX in DCM, DOX-EPT addition was performed in phosphate buffer. The emission peak of EPT around 530 nm, corresponding to the protonated form, was found to get quenched with progressive addition of DOX, similar to the emission profile of EPT with DOX-HNT addition (**Fig. 16**). At higher concentrations of DOX (~30  $\mu$ l), the emission profile of the system shifts more towards the emission spectra of DOX with the peaks around 560 nm and 590 nm getting more prominent, suggesting that the EPT emission is more or less completely quenched. Comparing the emission spectra of EPT-DOX and EPT, we can conclude that the quenching of EPT with addition of DOX-HNT was indeed caused by the interaction between EPT and DOX. Overall observation is that, during loading of EPT in DOX-HNT system, both EPT and DOX interacts with each other; however, such interactions between the drug molecules can lead to complications and makes the Halloysite less attractive as a dual drug carrier.

## Conclusion

In this work, we have performed loading of an another anticancer drug, Doxorubicin (DOX) onto hallosite nanotubes (HNTs), and it has been observed that the drug was mostly loaded inner lumen and a few drug molecules are loaded on the external surface of HNT. Confirmation of drug loading was obtained through steady-state fluorescence measurements in which the emission of DOX was getting quenched with HNT addition. The gas adsorption study confirms the loading of drug molecules into the inner lumen of HNT as the pore size and volume decrease after loading of the drug. On the other hand the TEM images of the sample show thickening of both internal and external surface of HNT, implying the presence of drug molecules on both surfaces. Zeta potential of DOX-HNT remained more or less same as that of HNT alone, suggesting DOX molecules mostly occupy the inner lumen of HNT. As the outside surface of HNT is mostly unoccupied, there is a possibility of loading Ellipticine (EPT) on DOX loaded HNT, i.e., DOX-HNT system. Emission spectra of EPT was

found to quench upon addition of DOX-HNT in DCM and no switching from neutral to protonated form of EPT was observed. The absence of any switching was attributed to the effect of basic environment on HNT surface where hydroxyl groups exist in the deprotonated form and the quenching of EPT emission was also not observed when treated HNT was added to EPT. Thus, the quenching of EPT emission can be attributed to the interactions between EPT and DOX in DOX-HNT. However, drug-drug interactions might lead to complications and is undesirable in a dual drug carrier. Therefore, HNT system is not an ideal carrier for dual delivery of both EPT and DOX.



### **3.3. Formation of Composite Material between HNT and GO and its Application Towards Dual Drug Loading**

In the previous chapter, possibility of achieving dual drug delivery of Ellipticine and Doxorubicin in pristine Halloysite was explored by loading EPT and DOX on external surface and inner lumen, respectively. However, interaction between DOX and EPT were observed when loaded onto HNT, and this is undesirable since it can lead to complications. Therefore, in this work, composite material of Halloysite and Graphene Oxide (GO) was synthesised, and the possibility of dual drug loading was explored. Graphene Oxide (GO) is a derivative of Graphene, a two dimensional planar sheet with monolayer of single atom thickness. GO consists of domains of  $sp^2$  carbon atoms packed in regular hexagonal pattern, similar to that of graphene, surrounded by  $sp^3$  carbon domains with various oxygen-containing functional groups such as epoxide, hydroxyl, carbonyl and carboxyl.<sup>42</sup> High surface area, water solubility, biocompatibility and presence of polar groups and  $\pi$  conjugation makes GO a suitable choice for drug delivery applications.<sup>17</sup> Loading of various therapeutic agents including Ellipticine and Doxorubicin has already been explored.<sup>17, 43-45</sup> Moreover, the presence of  $-COOH$  and  $-OH$  functional groups in GO enables conjugation with other systems.

We are expecting in a composite material of HNT and GO (both of which are capable of loading EPT and DOX individually), the drugs occupy two different carriers according to the affinity of the drugs, thus minimising the chances of drug-drug interaction. With the prior intuition, we are trying to explore the loading of two different anticancer drugs (EPT and DOX) to the composite material separately as well as together. The composite material was synthesised by first modifying HNT to amine functionalised HNT (HNT-NH<sub>2</sub>) and linking to the carboxyl groups of GO via amide bond formation.

#### **Experimental Section**

Halloysite nanotubes, graphite flakes, ethylenediamine (EDA), 2-(N-Morpholino) ethanesulfonic acid (MES) hydrate N-(3-Dimethylaminopropyl)-N'

ethylcarbodiimide hydrochloride (EDC), N-Hydroxysuccinimide (NHS) and Doxorubicin hydrochloride were purchased from Sigma-Aldrich. Epichlorohydrin and Ellipticine were purchased from TCI Chemicals and Cayman Chemicals, respectively. All the reagents were used without further purification. Molecular biology grade potassium phosphate monobasic and sodium phosphate dibasic were obtained from Sisco Research Laboratories (SRL India). Stock solution of DOX and EPT were prepared in Millipore water and DMSO, respectively. The drug loading experiments were performed in 10 mM phosphate buffer (pH=7).

### **Synthesis of Graphene Oxide**

GO was synthesized from graphite flakes using modified Hummers' method.<sup>46</sup> 2 g of powdered graphite flake was stirred with 40 mL of concentrated H<sub>2</sub>SO<sub>4</sub> at around 5°C for 1 hour and 6 g of KMnO<sub>4</sub> was added slowly for about half hour. The mixture was stirred for 24 hours at room temperature. 80 mL of Millipore water was added to the mixture with stirring and the mixture was stirred for 3 hours at 80°C and was allowed to reach back to room temperature. 20 mL H<sub>2</sub>O<sub>2</sub>, 240 mL H<sub>2</sub>O was added to the mixture and left for few hours. The material was then washed with H<sub>2</sub>O, 5% HCl solution and acetone and was then dried under vacuum at 70°C overnight.

### **Preparation of amine functionalised Halloysite**

The NaOH treated HNT (HNT-Na) was washed several times with water till the pH of the supernatant solution becomes neutral pH, to remove NaOH residuals. 1.5 g of HNT-Na was dispersed in 55 mL DMF in a 100 mL round bottom flask, and a good dispersion was obtained by stirring the mixture at 500 rpm for 20 minutes at room temperature. The flask was then immersed in oil bath of 90°C for 10 minutes to equate the temperature. 0.04 mole of epichlorohydrin was added to the dispersion and with the stirring at 750 rpm continued for one more hour. 0.04 mole of ethylenediamine dissolved in 5 mL DMF was then added to the mixture drop wise, and the reaction was allowed to continue for an hour after the last drop was added. The final product was centrifuged at 7,000 rpm and washed once with DMF and thrice with 1:1 v/v ethanol water mixture to remove unreacted reagents. The purified product was then dried in vacuum overnight. The synthesis has been performed following the protocol of Nurettin *et al.*<sup>47</sup>

## Synthesis of HNT-GO composite material

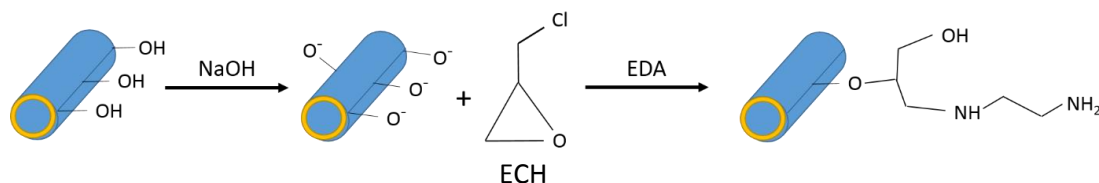
100mg of GO was added to 150 mL of water and subjected to 3 hour sonication to exfoliate GO. 60 mg of EDC and 48 mg of NHS were added to the solution. To keep the solution pH around 5, MES was added followed by stirring for 30 minutes and sonication for 30 minutes to form a homogenous suspension. 100 mg of HNT-NH<sub>2</sub> was added into the suspension and was sonicated for 30 minutes. The coupling was carried out at 80°C for 1 hours under stirring condition. The final composite was collected after centrifugation and was washed several times with Millipore water to remove unreacted GO sheets.

0.3 mg/mL stock solution of HNT-GO composite was used for all drug loading experiments. The solution was strongly sonicated before being added to drug solution.

## Results and Discussion

### Modification of HNT and Synthesis of HNT-GO Composite Material

Functionalization of HNT was achieved by reacting HNT with epichlorohydrin (ECH), followed by addition of ethylenediamine (EDA) (**scheme 4**) Treatment of HNT with NaOH can etch the siloxane surface and form Si-OH groups whereas high concentration of NaOH can result in significant structural changes and dissolution. Therefore, HNT was initially treated with 0.1 M NaOH for half hour at room temperature to increase the density of silanol groups, which will react with ECH for further modification. The ECH treated HNT was then modified to amine functionalised HNT



**Scheme 4.** Modification of HNT to HNT-NH<sub>2</sub>.



**Scheme 5.** Synthesis of HNT-GO composite material.

(HNT-NH<sub>2</sub>) with the addition of EDA. HNT-NH<sub>2</sub> attached to GO by making linkage via EDC/NHS coupling reaction carried out at 80 °C (**Scheme 5**). To achieve higher efficiency, MES buffer of pH 5 was used instead of phosphate buffer.

## Characterisation

FT-IR spectra of HNT and HNT-NH<sub>2</sub> are provided in **Figure 18**. The peaks assignment has been done based on the work of Yuan *et al.*<sup>22</sup> The peak at 524 cm<sup>-1</sup>

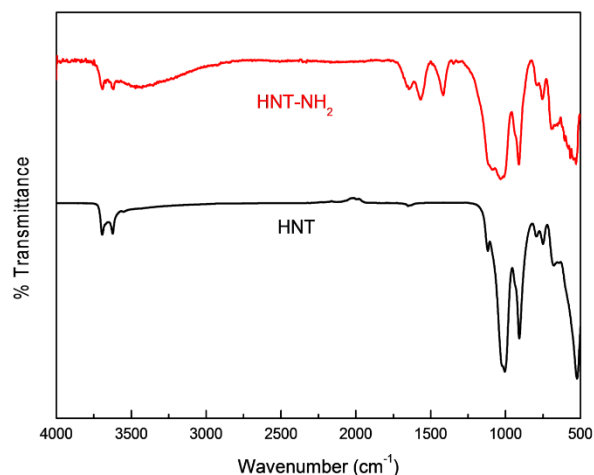


**Fig 18.** FT-IR spectra of HNT and modified HNT (HNT-NH<sub>2</sub>).

in the HNT IR spectra can be assigned to Al-O-Si deformation, whereas the peaks at 750 and 795 cm<sup>-1</sup> are due to perpendicular stretching and symmetric stretching of Si-O, respectively. 910 cm<sup>-1</sup> peak is assigned to the deformation of the inner hydroxyl groups of lumen and that around 1010 cm<sup>-1</sup> is attributed to Si-O stretching. The peaks at 3624 and 3694 cm<sup>-1</sup> are the stretching vibrations of Al-OH bonds. Apart from the presence of

all the above mentioned peaks, HNT-NH<sub>2</sub> spectra consists of new peaks at 1416 cm<sup>-1</sup>, 1564 cm<sup>-1</sup> and around 3400 cm<sup>-1</sup>. The peaks at 1416 and 1564 cm<sup>-1</sup> can be assigned to the bending frequencies of CH<sub>2</sub> and NH<sub>2</sub>, respectively. The broad peak around 3400 cm<sup>-1</sup> can be due to stretching of N-H and O-H bonds in amine and water present in the sample.<sup>22, 48</sup> Hence, the presence of additional peaks in HNT-NH<sub>2</sub> confirms the successful modification of HNT. The zeta potential measurement was also found to vary after modification of HNT (**Table 6**). Surface charge of HNT changed from -34 mV to -16 mV. The drop in the negative value of the zeta potential of HNT can attributed to the functionalization of amine groups at outer surface. However, the modified HNT was found to have lower surface area and pore volume than pure HNT (**Table 6**). Thus, the reduction can be attributed to the amine functionalization to the inner lumen hydroxyl groups, which can block the pores resulting in lower surface area and pore volume.

The composite material (HNT-GO) was characterised mainly through FESEM imaging, TGA and FT-IR spectra. FE-SEM images of HNT, GO and HNT-GO composite material are provided in **Fig. 19**. The tubular morphology with high aspect

**Table 6:** Porous structural data and Zeta potentials of HNT and modified HNT (HNT-NH<sub>2</sub>).

Sample	S <sub>BET</sub> (m <sup>2</sup> /g)	Pore volume (cm <sup>3</sup> /g)	Zeta potential (mV)
HNT	57.835	0.300	-34.54 ± 2.45
HNT-NH <sub>2</sub>	43.238	0.261	-16.32 ± 0.79

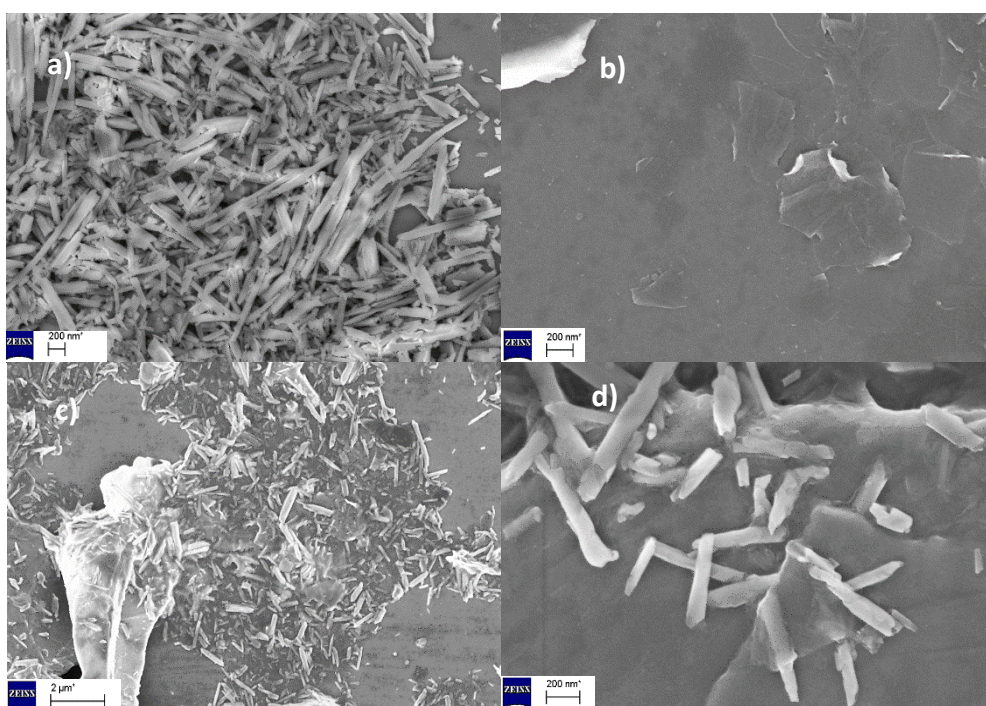


**Fig 19.** FE-SEM images of a) HNT b) GO and (c,d) HNT-GO.

ratio of HNT is evident (**Fig. 19a**). From the FE-SEM image (**Fig. 19b**), the platelets of GO can be identified. In the images of composite material, the tubular HNT is being attached to the planar GO surface (**Fig. 19c,d**). Moreover, from the images, it is evident that the morphology of both HNT and GO was preserved in the composite

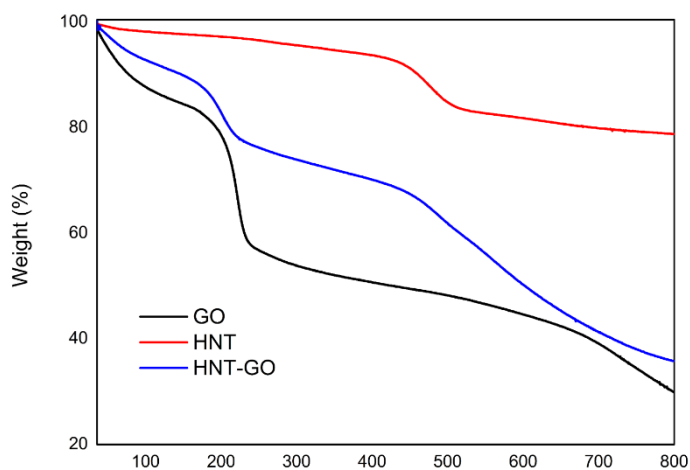


**Fig 20.** TGA thermograms of GO, HNT and HNT-GO.

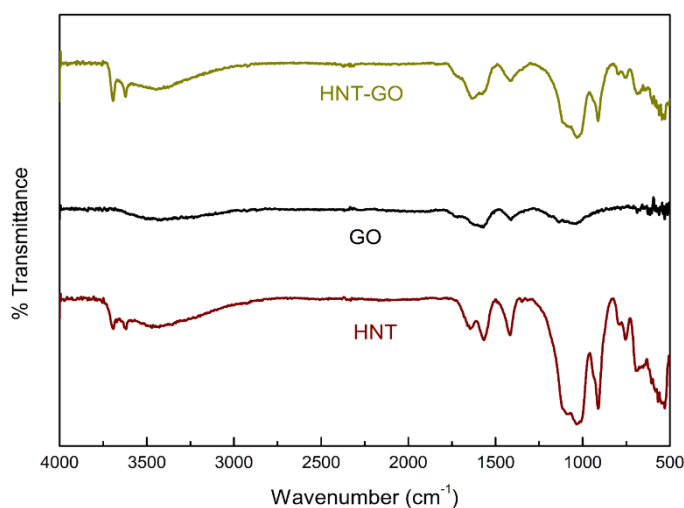


**Fig 21.** FT-IR spectra of HNT-NH<sub>2</sub>, GO and HNT-GO.

IR spectra of GO contains peak around 1048 cm<sup>-1</sup>, 1585 cm<sup>-1</sup>, 1730 cm<sup>-1</sup> and 3440 cm<sup>-1</sup> which can be assigned to the stretching vibrations of epoxide or alkoxy -C-O, graphene C=C, carbonyl moiety in -COOH and -OH respectively (**Fig. 21**). FT-IR spectra of HNT-NH<sub>2</sub> is explained previously. The IR spectra of HNT-GO composite material contains all the peaks corresponding to the modified HNT, which confirms the presence of HNT in the composite material. When the FT-IR spectra of HNT-GO compared with that of HNT-NH<sub>2</sub>, a new peak around 1710 cm<sup>-1</sup> is observed, and this can be attributed to the stretching vibration of C=O group. Although the frequency of C=O stretch (1710 cm<sup>-1</sup>) is lower than that found in GO (1730 cm<sup>-1</sup>), the value is still higher than what is expected for amide II band (less than 1700 cm<sup>-1</sup>). The anomaly might due to presence of unreacted -COOH groups still present in the composite

material. TGA data for HNT, GO and HNT-GO is provided in **Fig. 20**. Initial drop in the weight of GO around 100°C is mostly due to the loss of water molecules in the GO layers. The second major loss of about 35% near 225°C can be attributed to the decomposition of oxygen-containing functional groups of GO and the final weight loss around 650°C is due to the combustion of the carbon skeleton.<sup>49</sup> In the case of HNT, the weight loss at 430°C-500°C region is due to the dehydroxylation of structurally bonded water.<sup>50</sup> In the TGA profile of the composite material (HNT-GO), weight loss corresponding to both GO and HNT were observed, thus, confirming the presence of both the components in HNT-GO. FT-

material. Thus, the FT-IR data cannot confirm the formation of amide bond in the HNT-GO, and needs to be redone. The formation of amide bond needs to be further confirmed through other techniques, such as  $^{15}\text{N}$  and proton NMR.

### Loading Ellipticine onto Composite Material

The loading of EPT to the composite material (HNT-GO) was performed in phosphate buffer. In the aqueous media, EPT exists in its protonated form, having emission peak around 530 nm (**Fig. 22a**). With the addition of composite material, the

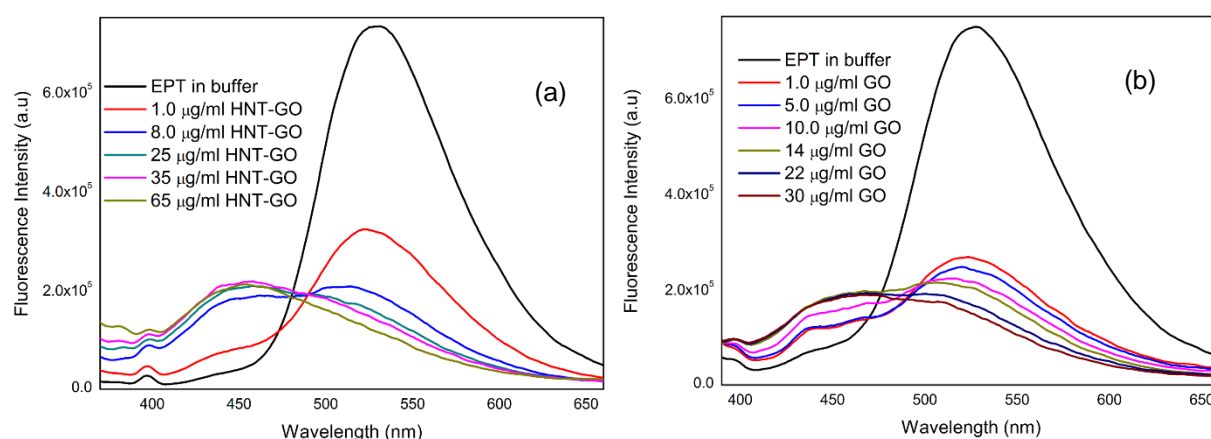


**Fig 22.** Emission spectra of EPT in buffer with gradual addition of (a) the composite material and (b) graphene oxide ( $\lambda_{\text{ex}} = 350$  nm).

530 nm peak is getting diminished along with gradual growth of a new peak around 450 nm. The switching of emission spectra of EPT confirms that EPT molecules bind to the composite material. In the previous chapter, we have already observed that when EPT binds to HNT in buffer, no fluorescence switching takes place, since EPT already exists in the protonated form in buffer. Moreover, fluorescence switching (from green to blue) of EPT takes place in presence of GO (**Fig. 22b**). The similarity in emission profile of EPT in the case of HNT-GO and GO suggests that the EPT is binding to the GO surface rather than to HNT.

### Loading Doxorubicin onto Composite Material

Emission spectra of DOX in buffer was found to get quenched with gradual addition of the composite material (**Fig. 23**). In the previous chapter, we have seen that the DOX emission was quenched with HNT addition due to electron transfer from DOX to HNT. The quenching of DOX emission also takes place when loaded onto GO, due to  $\pi$ - $\pi$  stacking interaction between the two.<sup>51</sup> Since both the components of the

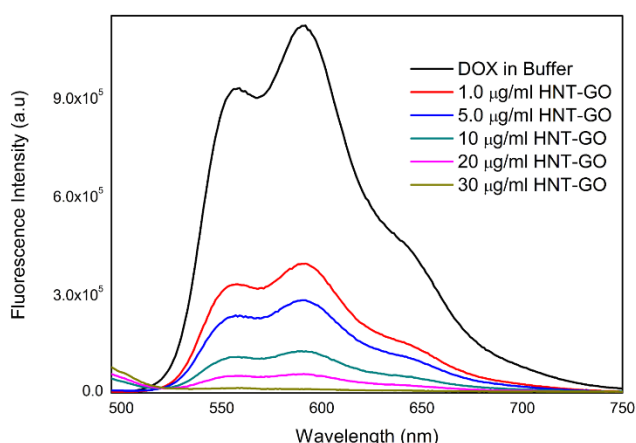


**Fig 23.** Emission spectra of DOX in buffer with gradual addition of graphene oxide ( $\lambda_{ex} = 470$  nm).

composite material individually can cause quenching to DOX emission, it is not possible to distinguish whether the drug is loaded onto the GO or HNT surface. Overall, the quenching of the emission indicates loading of DOX onto HNT-GO.

### Dual Drug loading onto Composite Material

Since EPT and DOX were found to be capable of loading onto the composite material individually, the possibility of dual drug delivery was explored. For achieving dual loading, DOX was added onto EPT loaded HNT-GO system (EPT-HNT-GO), and was monitored through fluorescence spectra (**Fig. 24**). EPT loaded onto the composite material exhibits a peak around 450 nm corresponding to the neutral form of EPT attached to the GO surface. Now, when DOX is added to the EPT loaded HNT-GO system, the 450 nm peak was found to be undisturbed (**Fig. 24a**). In the previous chapter, it is already shown that EPT-DOX interaction can quench EPT emission. The absence of any significant reduction in emission intensity at 450 nm suggests that there is no interaction between EPT bound to the HNT-GO and DOX molecules. From the emission spectra of EPT, it is hard to confirm whether DOX is getting loaded on EPT-HNT-GO system or not. To verify the loading of DOX to the system, emission spectrum of DOX has been probed. The

Since EPT and DOX were found

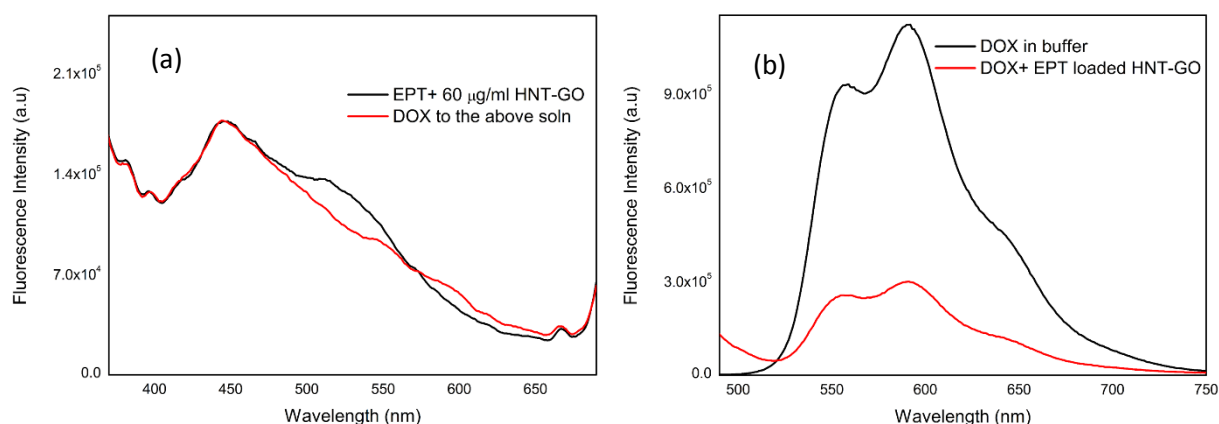


**Fig 24.** Emission spectra of a) EPT loaded onto HNT-GO, before and after DOX addition ( $\lambda_{ex} = 350$  nm) b) DOX in buffer, before and after addition of EPT loaded HNT-GO ( $\lambda_{ex} = 470$  nm).



emission intensity of DOX was found to get reduced when added to EPT-HNT-GO system (**Fig. 24b**). Since we have already seen that quenching of DOX emission indicates DOX loading onto HNT-GO, from this emission spectra, we can confirm that DOX is indeed getting loaded onto EPT-HNT-GO. Overall, the emission studies confirm that both the drugs are being loaded onto the composite material. The absence of any interaction between the drug molecules (unlike in the case of dual drug loaded onto HNT), makes the composite material of HNT and GO, a better choice than pristine HNT for dual drug delivery of DOX and EPT.

## **Conclusion**

In this study, composite material of halloysite (HNT) and graphene oxide (GO) was synthesised. This was achieved by modifying HNT to HNT-NH<sub>2</sub> and then making amide bond with –COOH groups of GO. The modified HNT and the composite material was characterised through various techniques, like, FT-IR, FE-SEM, zeta potential and gas adsorption-desorption measurements. Before exploring the possibility of dual drug loading, capability of Ellipticine (EPT) and Doxorubicin (DOX) to bind with the composite material (HNT-GO) was investigated. EPT in buffer was found to convert to the neutral form in HNT-GO system, indicated by the switching of emission from 530 nm to 450 nm. This emission profile is similar to that of EPT loading onto GO, suggesting that the EPT molecules are binding to GO surface in HNT-GO. Quenching of DOX emission was observed upon addition of HNT-GO. Since GO and HNT individually cause quenching of DOX emission, it is not possible to distinguish actual site of interaction within HNT-GO. To achieve dual drug loading, DOX was added to EPT loaded HNT-GO. Loading of DOX onto the system was confirmed by reduction in emission intensity of DOX. Emission peak of EPT was found to be undisturbed after DOX addition, implying the absence of interaction between the two drugs, and makes the HNT-GO, a better carrier than pristine HNT for dual drug delivery of DOX and EPT.

## 4. Conclusion

In section 3.1, an anticancer drug Ellipticine (EPT) was successfully loaded onto the Halloysite nanotubes (HNT). The drug loading was confirmed through the switching in emission of EPT in DCM from blue to green corresponding to neutral and protonated form when loaded onto HNT. From the emission features, it is evident that the cationic EPT molecules are attached to the negatively charged external surface of HNT. Drug loading was also confirmed through various characterisation techniques such as confocal microscopy imaging, zeta potential measurements, gas adsorption studies and time-resolved fluorescence measurements. After loading EPT onto HNT, drug release was monitored in presence of DNA by steady-state fluorescence, time-resolved fluorescence and circular dichroism studies.

In the next section, another anticancer drug, Doxorubicin (DOX) was loaded onto HNT. In contrast to earlier reports, the DOX molecules were loaded mainly into the inner lumen, since the loading was performed in pH 8.6 condition, in which the DOX molecules exist predominantly in the neutral form. The drug loading was confirmed by the quenching of DOX emission with the addition of HNT, which can be attributed to the electron transfer from DOX to the empty orbitals of Aluminium present in the HNT surface. DOX loaded HNT was further characterised through zeta potential, gas adsorption and HR-TEM imaging techniques. Then, the possibility of loading both EPT and DOX simultaneously onto HNT was also explored. However, the indications of interactions between EPT and DOX when loaded onto HNT, makes pristine HNT not suitable for dual drug loading.

In order to circumvent above mentioned problem related to dual drug delivery using HNT alone, a composite material of HNT and Graphene Oxide (GO) was synthesised. This was achieved by first functionalising HNT to HNT-NH<sub>2</sub>, followed by amide linkage with –COOH groups of GO. Modified HNT and the composite material (HNT-GO) were characterised through various techniques such as FT-IR spectroscopy, TGA and FE-SEM imaging. Then, loading of EPT and DOX to the composite material was studied separately. The switching of EPT emission from green

to blue indicated that the EPT molecules are being attached to the GO surface of HNT-GO. Although DOX loading on composite material was confirmed using fluorescence measurements, the binding site of DOX could not be distinguished, since GO and HNT separately cause quenching to the DOX emission. Interestingly, no interaction between DOX and EPT molecules were observed when both the drugs were loaded onto HNT-GO. Therefore, the composite material of HNT and GO is found to be more suitable for the dual delivery of DOX and EPT than pristine HNT.

## Future Directions

The synthesised composite material of HNT and GO has to be thoroughly characterised using various techniques such as proton NMR, <sup>15</sup>N NMR, Raman spectroscopy and XRD. Dual loading of DOX and EPT to the composite, performed in section 3.3, needs to be scaled up, to obtain drug loaded samples in milligram or gram scale. The interaction of the dual drug loaded HNT-GO with various biomolecules like DNA and proteins needs to be explored in detail. The next step would be to monitor the cellular uptake and drug release inside cellular environment. Since DOX and EPT has well separated emission peaks, the release studies of each drug can be distinguished and monitored through confocal imaging microscopy. For application of HNT-GO as a drug carrier, cytotoxicity and biocompatibility of the material needs to be evaluated as well. Moreover, our exploration of HNT-GO as a carrier for dual loading of DOX and EPT, paves the way of application of the composite material for dual delivery of other important drug molecules.

## References

1. Dai, L.; Liu, J.; Luo, Z.; Li, M.; Cai, K., Tumor Therapy: Targeted Drug Delivery Systems. *Journal of Materials Chemistry B* **2016**, *4*, 6758.
2. Lvov, Y. M.; Shchukin, D. G.; Möhwald, H.; Price, R. R., Halloysite Clay Nanotubes for Controlled Release of Protective Agents. *ACS Nano* **2008**, *2*, 814.
3. Lvov, Y.; Wang, W.; Zhang, L.; Fakhrullin, R., Halloysite Clay Nanotubes for Loading and Sustained Release of Functional Compounds. *Advanced Materials* **2016**, *28*, 1227.
4. Yuan, P.; Tan, D.; Annabi-Bergaya, F., Properties and Applications of Halloysite Nanotubes: Recent Research Advances and Future Prospects. *Applied Clay Science* **2015**, *112-113*, 75.
5. Tully, J.; Yendluri, R.; Lvov, Y., Halloysite Clay Nanotubes for Enzyme Immobilization. *Biomacromolecules* **2016**, *17*, 615.
6. Lee, Y.; Jung, G.-E.; Cho, S. J.; Geckeler, K. E.; Fuchs, H., Cellular Interactions of Doxorubicin-loaded DNA-modified Halloysite Nanotubes. *Nanoscale* **2013**, *5*, 8577.
7. Levis, S. R.; Deasy, P. B., Use of Coated Microtubular Halloysite for the Sustained Release of Diltiazem Hydrochloride and Propranolol Hydrochloride. *Int J Pharm* **2003**, *253*, 145.
8. Massaro, M.; Cavallaro, G.; Colletti, C. G.; Lazzara, G.; Milioto, S.; Noto, R.; Riela, S., Chemical Modification of Halloysite Nanotubes for Controlled Loading and Release. *Journal of Materials Chemistry B* **2018**, *6*, 3415.
9. Yah, W. O.; Takahara, A.; Lvov, Y. M., Selective Modification of Halloysite Lumen with Octadecylphosphonic Acid: New Inorganic Tubular Micelle. *Journal of the American Chemical Society* **2012**, *134*, 1853.
10. Liu, F.; Bai, L.; Zhang, H.; Song, H.; Hu, L.; Wu, Y.; Ba, X., Smart H<sub>2</sub>O<sub>2</sub>-Responsive Drug Delivery System Made by Halloysite Nanotubes and Carbohydrate Polymers. *ACS Applied Materials & Interfaces* **2017**, *9*, 31626.
11. Zhao, Y.; Abdullayev, E.; Vasiliev, A.; Lvov, Y., Halloysite Nanotubule Clay for Efficient Water Purification. *Journal of Colloid and Interface Science* **2013**, *406*, 121
12. Gavvala, K.; Sengupta, A.; Koninti, R. K.; Hazra, P., Prototypical and Photophysical Properties of Ellipticine inside the Nanocavities of Molecular Containers. *The Journal of Physical Chemistry B* **2013**, *117*, 14099.
13. Le Pecq, J. B.; Nguyen Dat, X.; Gosse, C.; Paoletti, C., A New Antitumoral Agent: 9-Hydroxyellipticine. Possibility of a Rational Design of Anticancerous Drugs in the Series of DNA Intercalating Drugs. *Proceedings of the National Academy of Sciences of the United States of America* **1974**, *71*, 5078.
14. Sureau, F.; Moreau, F.; Millot, J. M.; Manfait, M.; Allard, B.; Aubard, J.; Schwaller, M. A., Microspectrofluorometry of the Protonation State of Ellipticine, an Antitumor Alkaloid, in Single Cells. *Biophysical journal* **1993**, *65*, 1767.
15. Fung, S. Y.; Duhamel, J.; Chen, P., Solvent Effect on the Photophysical Properties of the Anticancer Agent Ellipticine. *The Journal of Physical Chemistry A* **2006**, *110*, 11446.
16. Koninti, R. K.; Palvai, S.; Satpathi, S.; Basu, S.; Hazra, P., Loading of An Anti-cancer Drug into Mesoporous Silica Nano-Channels and Its Subsequent Release to DNA. *Nanoscale* **2016**, *8*, 18436.

17. Koninti, R. K.; Sengupta, A.; Gavvala, K.; Ballav, N.; Hazra, P., Loading of an Anti-Cancer Drug onto Graphene Oxide and Subsequent Release to DNA/RNA: A Direct Optical Detection. *Nanoscale* **2014**, *6* (5), 2937.
18. Sbai, M.; Ait Lyazidi, S.; Lerner, D. A.; del Castillo, B.; Martin, M. A., Use of Micellar media for the Fluorimetric Determination of Ellipticine in Aqueous Solutions. *Journal of Pharmaceutical and Biomedical Analysis* **1996**, *14*, 959.
19. Thakur, R.; Das, A.; Chakraborty, A., Fate of Anticancer Drug Ellipticine in Reverse Micelles in Aqueous and Methanolic Environment: A Photophysical Approach. *Chemical Physics Letters* **2013**, *563*, 37.
20. Gavvala, K.; Satpathi, S.; Hazra, P., pH Responsive Translocation of an Anticancer Drug Between Cyclodextrin and DNA. *RSC Advances* **2015**, *5*, 98080.
21. Ong, S.; Zhao, X.; Eisenthal, K. B., Polarization of Water Molecules at a Charged Interface: Second Harmonic Studies of the Silica/Water Interface. *Chemical Physics Letters* **1992**, *191*, 327.
22. Yuan, P.; Southon, P. D.; Liu, Z.; Green, M. E. R.; Hook, J. M.; Antill, S. J.; Kepert, C. J., Functionalization of Halloysite Clay Nanotubes by Grafting with  $\gamma$ -Aminopropyltriethoxysilane. *The Journal of Physical Chemistry C* **2008**, *112*, 15742.
23. Barrett, E. P.; Joyner, L. G.; Halenda, P. P., The Determination of Pore Volume and Area Distributions in Porous Substances. I. Computations from Nitrogen Isotherms. *Journal of the American Chemical Society* **1951**, *73*, 373.
24. Yuan, P.; Tan, D.; Aannabi-Bergaya, F.; Yan, W.; Fan, M.; Liu, D.; He, H., Changes in Structure, Morphology, Porosity, and Surface Activity of Mesoporous Halloysite Nanotubes Under Heating. *Clays and Clay Minerals* **2012**, *60*, 561.
25. Sengupta, A.; Koninti, R. K.; Gavvala, K.; Ballav, N.; Hazra, P., An Anticancer Drug to Probe Non-Specific Protein–DNA Interactions. *Physical Chemistry Chemical Physics* **2014**, *16*, 3914.
26. Lee, W. L.; Guo, W. M.; Ho, V. H. B.; Saha, A.; Chong, H. C.; Tan, N. S.; Widjaja, E.; Tan, E. Y.; Loo, S. C. J., Inhibition of 3-D Tumor Spheroids by Timed-Released Hydrophilic and Hydrophobic Drugs from Multilayered Polymeric Microparticles. *Small* **2014**, *10*, 3986.
27. Lehár, J.; Krueger, A. S.; Avery, W.; Heilbut, A. M.; Johansen, L. M.; Price, E. R.; Rickles, R. J.; Short lli, G. F.; Staunton, J. E.; Jin, X.; Lee, M. S.; Zimmermann, G. R.; Borisy, A. A., Synergistic Drug Combinations Tend to Improve Therapeutically Relevant Selectivity. *Nature Biotechnology* **2009**, *27*, 659.
28. Ahmed, F.; Pakunlu, R. I.; Brannan, A.; Bates, F.; Minko, T.; Discher, D. E., Biodegradable Polymersomes Loaded with Both Paclitaxel and Doxorubicin Permeate and Shrink Tumors, Inducing Apoptosis in Proportion to Accumulated Drug. *Journal of Controlled Release* **2006**, *116*, 150.
29. Mohan, P.; Rapoport, N., Doxorubicin as a Molecular Nanotheranostic Agent: Effect of Doxorubicin Encapsulation in Micelles or Nanoemulsions on the Ultrasound-Mediated Intracellular Delivery and Nuclear Trafficking. *Molecular Pharmaceutics* **2010**, *7*, 1959.
30. Thorn, C. F.; Oshiro, C.; Marsh, S.; Hernandez-Boussard, T.; McLeod, H.; Klein, T. E.; Altman, R. B., Doxorubicin Pathways: Pharmacodynamics and Adverse Effects. *Pharmacogenetics and genomics* **2011**, *21*, 440.
31. Pommier, Y.; Leo, E.; Zhang, H.; Marchand, C., DNA Topoisomerases and Their Poisoning by Anticancer and Antibacterial Drugs. *Chemistry & Biology* **2010**, *17*, 421.
32. Yu, C.; Zhou, Q.; Xiao, F.; Li, Y.; Hu, H.; Wan, Y.; Li, Z.; Yang, X., Enhancing Doxorubicin Delivery Toward Tumor by Hydroxyethyl Starch-g-Polylactide Partner Nanocarriers. *ACS Applied Materials & Interfaces* **2017**, *9*, 10481.

33. Anand, R.; Ottani, S.; Manoli, F.; Manet, I.; Monti, S., A Close-up on Doxorubicin Binding to  $\gamma$ -Cyclodextrin: an Elucidating Spectroscopic, Photophysical and Conformational Study. *RSC Advances* **2012**, *2*, 2346.
34. Li, L.; Fan, H.; Wang, L.; Jin, Z., Does Halloysite Behave Like an Inert Carrier for Doxorubicin? *RSC Advances* **2016**, *6*, 54193.
35. Wolski, P.; Nieszporek, K.; Panczyk, T., Pegylated and Folic Acid Functionalized Carbon Nanotubes as pH Controlled Carriers of Doxorubicin. Molecular Dynamics Analysis of the Stability and Drug Release Mechanism. *Physical Chemistry Chemical Physics* **2017**, *19*, 9300.
36. Veerabadran, N. G.; Price, R. R.; Lvov, Y. M., Clay Nanotubes for Encapsulation and Sustained Release of Drugs. *Nano* **2007**, *2*, 115.
37. Bretti, C.; Cataldo, S.; Gianguzza, A.; Lando, G.; Lazzara, G.; Pettignano, A.; Sammartano, S., Thermodynamics of Proton Binding of Halloysite Nanotubes. *Journal of Physical Chemistry C* **2016**, *120*, 7849.
38. Liu, M.; Guo, B.; Du, M.; Jia, D., The Role of Interactions Between Halloysite Nanotubes and 2,2'-(1,2-Ethenediyl-di-4,1-phenylene) Bisbenzoxazole in Halloysite Reinforced Polypropylene Composites. *Polymer Journal* **2008**, *40*, 1087.
39. Liu, M.; Guo, B.; Zou, Q.; Du, M.; Jia, D., Interactions Between Halloysite Nanotubes and 2,5-bis(2-benzoxazolyl) Thiophene and Their Effects on Reinforcement of Polypropylene/Halloysite Nanocomposites. *Nanotechnology* **2008**, *19*, 205709.
40. Lakowicz, J. R., *Principles of Fluorescence Spectroscopy*. 3rd ed.; Springer: 2006.
41. Shah, S.; Chandra, A.; Kaur, A.; Sabnis, N.; Lacko, A.; Gryczynski, Z.; Fudala, R.; Gryczynski, I., Fluorescence Properties of Doxorubicin in PBS Buffer and PVA films. *Journal of Photochemistry and Photobiology B: Biology* **2017**, *170*, 65.
42. Loh, K. P.; Bao, Q.; Eda, G.; Chhowalla, M., Graphene Oxide as a Chemically Tunable Platform for Optical Applications. *Nature Chemistry* **2010**, *2*, 1015.
43. Liu, Z.; Liu, J.; Wang, T.; Li, Q.; Francis, P. S.; Barrow, C. J.; Duan, W.; Yang, W., Switching off the Interactions Between Graphene Oxide and Doxorubicin Using Vitamin C: Combining Simplicity and Efficiency in Drug Delivery. *Journal of Materials Chemistry B* **2018**, *6*, 1251.
44. Chung, C.; Kim, Y.-K.; Shin, D.; Ryoo, S.-R.; Hong, B. H.; Min, D.-H., Biomedical Applications of Graphene and Graphene Oxide. *Accounts of Chemical Research* **2013**, *46*, 2211.
45. Mao, H. Y.; Laurent, S.; Chen, W.; Akhavan, O.; Imani, M.; Ashkarran, A. A.; Mahmoudi, M., Graphene: Promises, Facts, Opportunities, and Challenges in Nanomedicine. *Chemical Reviews* **2013**, *113*, 3407.
46. Jha, P. K.; Singh, S. K.; Kumar, V.; Rana, S.; Kurungot, S.; Ballav, N., High-Level Supercapacitive Performance of Chemically Reduced Graphene Oxide. *Chem* **2017**, *3*, 846.
47. Sahiner, N.; Sengel, S. B., Various Amine Functionalized Halloysite Nanotube as Efficient Metal Free Catalysts for H<sub>2</sub> Generation From Sodium Borohydride Methanolysis. *Applied Clay Science* **2017**, *146*, 517.
48. Zhu, J.; Guo, N.; Zhang, Y.; Yu, L.; Liu, J., Preparation and Characterization of Negatively Charged PES Nanofiltration Membrane by Blending with Halloysite Nanotubes Grafted with Poly (sodium 4-styrenesulfonate) via Surface-Initiated ATRP. *Journal of Membrane Science* **2014**, *465*, 91.
49. Shen, J.; Hu, Y.; Li, C.; Qin, C.; Ye, M., Synthesis of Amphiphilic Graphene Nanoplatelets. *Small* **2009**, *5*, 82.

50. Ganguly, S.; Das, T. K.; Mondal, S.; Das, N. C., Synthesis of Polydopamine-Coated Halloysite Nanotube-based Hydrogel for Controlled Release of a Calcium Channel Blocker. *RSC Advances* **2016**, *6*, 105350.
51. Yang, X.; Zhang, X.; Liu, Z.; Ma, Y.; Huang, Y.; Chen, Y., High-Efficiency Loading and Controlled Release of Doxorubicin Hydrochloride on Graphene Oxide. *The Journal of Physical Chemistry C* **2008**, *112*, 17554.